Check for updates

JGR Biogeosciences

RESEARCH ARTICLE
10.1029/2025JG009061

Special Collection:
Exploring Carbon Cycling in Aquatic Ecosystems Using Novel Analytical and Data-Driven Approaches

Land Cover and Hydrology Regulate Riverine Carbon Emissions From Subarctic Catchments

T. Saarela[1], C. Palacin-Lizarbe[1,2], W. Hashmi[1], L. Kohl[1], M. E. Marushchak[1,3], H. M. P. Siljanen[1], X. Zhu[4], F. Berninger[4], and J. Pumpanen[1]

[1]Department of Environmental and Biological Sciences, University of Eastern Finland, Kuopio, Finland, [2]Center for Advanced Studies of Blanes (CEAB-CSIC), Blanes, Spain, [3]Department of Biological and Environmental Science, University of Jyväskylä, Jyväskylä, Finland, [4]Department of Environmental and Biological Sciences, University of Eastern Finland, Joensuu, Finland

Abstract Streams transport carbon (C) and nutrients across the terrestrial-aquatic interface and are significant sources of methane (CH_4) and carbon dioxide (CO_2) to the atmosphere. Climate-induced changes in vegetation and hydrology increase the export of dissolved organic carbon (DOC) from terrestrial to aquatic ecosystems, but the impact of these alterations on freshwater C gas emissions remains uncertain. We investigated the influence of landcover and hydrology on stream CH_4 and CO_2 fluxes in two subarctic catchments differing in vegetation and soil type by floating chamber measurements, stable isotope analyses of emitted CH_4 and CO_2, and microbial analyses of CH_4-related microbial communities. Monthly flux measurements and water and microbial sampling were performed from spring to fall during two growing seasons. The results reveal higher CH_4 and CO_2 fluxes from a brown-water stream surrounded by peatlands compared with a clear-water stream located in an upland mineral soil catchment. While CO_2 fluxes peaked during spring freshet in both streams, CH_4 dynamics showed distinct seasonal patterns between the streams. In the brown-water stream, the maximum CH_4 fluxes coincided with the spring peak in discharge and DOC, suggesting that the CH_4 fluxes were controlled by surface flow and DOC load from peatlands. In the clear-water stream, the maximum CH_4 fluxes detected during late summer were likely connected to rain events and shifting hydrological pathways during base flow. Furthermore, submerged vegetation and sediment surfaces contributed to CH_4 dynamics by providing important habitats for methanotrophic microbes. We highlight that landcover and hydrology regulate C gas fluxes from subarctic streams.

Plain Language Summary Streams transfer carbon and nutrients between land and water and release greenhouse gases such as methane (CH_4) and carbon dioxide (CO_2) into the air. Climate change is increasing the flow of dissolved organic carbon (DOC) from land to water, but it is unclear how this influences greenhouse gas emissions from streams. This study measured CH_4 and CO_2 emissions from two streams located in catchments dominated by either peatland or upland mineral soil from spring to fall over 2 years. We found that a stream surrounded by peatlands released more CH_4 and CO_2 than a stream located in uplands. CO_2 emissions were highest during spring in both streams, but CH_4 emissions differed between the streams. In the peatland stream, CH_4 emissions peaked in spring with high water flow and DOC levels, whereas in the upland stream, CH_4 emissions were highest in late summer due to rain events and changing water flow. We also found that aquatic plants and sediment surfaces can impact CH_4 emissions from streams by supporting methane-consuming microbes. This study shows that the land cover type and water flow play an important role in how much greenhouse gases are released from streams.

Key Points:

- Stream fluxes and stable isotope values of CH_4 and CO_2 were higher in peatland-dominated catchment compared with upland forest catchment
- DOC export, water discharge, and precipitation were the main factors predicting the seasonal patterns in CH_4 and CO_2 fluxes
- Submerged aquatic vegetation and surficial sediments are important habitats for methanotrophic microbes in both streams

Supporting Information:

Supporting Information may be found in the online version of this article.

Correspondence to:

T. Saarela,
taija.saarela@uef.fi

Citation:

Saarela, T., Palacin-Lizarbe, C., Hashmi, W., Kohl, L., Marushchak, M. E., Siljanen, H. M. P., et al. (2026). Land cover and hydrology regulate riverine carbon emissions from subarctic catchments. *Journal of Geophysical Research: Biogeosciences*, *131*, e2025JG009061. https://doi.org/10.1029/2025JG009061

Received 15 MAY 2025
Accepted 7 DEC 2025

Author Contributions:

Conceptualization: L. Kohl, F. Berninger, J. Pumpanen
Data curation: T. Saarela, C. Palacin-Lizarbe, H. M. P. Siljanen
Formal analysis: T. Saarela, C. Palacin-Lizarbe, W. Hashmi
Investigation: T. Saarela, C. Palacin-Lizarbe, W. Hashmi, X. Zhu, F. Berninger, J. Pumpanen

© 2025. The Author(s).
This is an open access article under the terms of the Creative Commons Attribution License, which permits use, distribution and reproduction in any medium, provided the original work is properly cited.

1. Introduction

Carbon (C) flux across terrestrial-aquatic interfaces has a major role in the overall C balance of ecosystems, and it is central to the biogeochemistry of recipient streams and rivers (Gómez-Gener et al., 2021). Streams are significant emitters of CO_2 and CH_4 to the atmosphere (Dinsmore et al., 2010; Raymond et al., 2013; Wallin et al., 2013), but current global estimates of CO_2 and CH_4 emissions from fluvial systems remain poorly quantified (Drake et al., 2018). Processes underlying CO_2 and CH_4 dynamics need to be better understood to develop process-based biogeochemical models predicting current and future greenhouse gas (GHG) emissions to the atmosphere (Riley et al., 2011).

Methodology: H. M. P. Siljanen
Resources: J. Pumpanen
Software: M. E. Marushchak, H. M. P. Siljanen
Supervision: J. Pumpanen
Validation: L. Kohl, H. M. P. Siljanen
Visualization: T. Saarela, C. Palacin-Lizarbe
Writing – original draft: T. Saarela
Writing – review & editing: T. Saarela, C. Palacin-Lizarbe, W. Hashmi, L. Kohl, M. E. Marushchak, H. M. P. Siljanen, X. Zhu, J. Pumpanen

Different forms of C, including dissolved organic carbon (DOC), particulate organic carbon (POC), and dissolved inorganic carbon (DIC), released from terrestrial ecosystems (e.g., forests and peatlands) vary in their chemical composition, reactivity, and seasonal patterns, and thus have distinct fates in downstream networks (Gómez-Gener et al., 2021). It is particularly important to assess different forms and fates of terrestrial C flux in heterogeneous northern landscapes that consist of forests, peatland mires and freshwaters and store large amounts of organic matter in soils (Bradshaw & Warkentin, 2015). This heterogeneity can create considerable variation in soil-stream interfaces that further regulate the timing and magnitude of C exchange to the atmosphere (Campeau et al., 2018; Gómez-Gener et al., 2021). Small streams have been found to be especially important in regional C cycling due to their significant contribution to C gas evasion (Huotari et al., 2013). Lateral C transport from soils to freshwater streams and lakes can account for 10%–50% of the terrestrial net ecosystem exchange (NEE) of old-growth forests and is particularly significant in peatland-dominated catchments (Juutinen et al., 2013; Olefeldt et al., 2013; Rasilo, 2013). Across northern landscapes, the export of DOC from terrestrial to aquatic ecosystems has been found to increase with increasing vegetation cover, changing hydrology, and reduced sulfate deposition (Asmala et al., 2019; Finstad et al., 2016; Monteith et al., 2007; Schuur et al., 2009). The increased delivery of terrestrial DOC might further accelerate the mineralization of DOC into greenhouse gases in aquatic ecosystems (Bayer et al., 2019; Berggren & Del Giorgio, 2015; Lapierre et al., 2013).

In addition to landscape and catchment characteristics, hydrological conditions also significantly influence C fluxes in northern ecosystems, regulating the biogeochemistry of downstream networks. Headwater streams in temperate and boreal landscapes are characterized by a strong seasonality in hydrological conditions, with maximum discharge occurring during the spring freshet and prolonged baseflow periods during the summer and winter (Fouché et al., 2017; Shogren et al., 2020). As climate change progresses, hydrologic intensification is projected to influence the timing and magnitude of high-flow events (McClelland et al., 2006; Peterson et al., 2002) and alter the export and availability of C compounds and nutrients in watercourses (Finlay et al., 2006; Guo et al., 2007; Wickland et al., 2018). Fluctuations in hydrological conditions might alter the dominant flow pathways through catchment soil horizons (Schelker et al., 2013) and impact the hydrologic connectivity of different landscape elements, such as soils, peatlands, and lakes (Laudon et al., 2011). Furthermore, groundwater discharge has been identified to be an important mechanism in C cycling of northern high-latitude freshwaters (Connolly et al., 2020; Walvoord & Striegl, 2007). Recent studies report that groundwater flow paths can release highly biolabile DOC (McDonough et al., 2022) and act as a source of CO_2 and CH_4 to streams (Biehler et al., 2023; Duvert et al., 2018; Lupon et al., 2019). However, increased groundwater to stream discharge during baseflow may result in decreased DOC concentrations compared with surface runoff (Walvoord & Striegl, 2007) because water draining from soil surfaces typically has high DOC concentrations compared with deeper soil water (Kawahigashi et al., 2006).

The biogeochemical transformations accompanying the transport of C from soils to streams remain inadequately determined (Campeau et al., 2017). Stable isotope analysis has been found to be a powerful tool for providing valuable insights into the sources, sinks, and transformations of CO_2 and CH_4 within terrestrial and aquatic ecosystems (Karlsson et al., 2007). The stable carbon isotopic signatures ($^{13}C/^{12}C$ ratio, commonly expressed with δ-notation as ‰-difference relative to the reference standard) can be used to determine the production, consumption, and transport of C within ecosystems (Chanton, 2005; Chanton et al., 2005), as well as to demonstrate seasonal and interannual changes in primary production and respiration (Yakir & Sternberg, 2000). Furthermore, stable carbon isotopes can be used in the identification of methanogenic pathways (Conrad, 2005). The ^{13}C values of CH_4 vary depending on its production pathway. Methane derived from H_2/CO_2 in hydrogenotrophic methanogenesis is generally more depleted in ^{13}C (−100 to −60‰) than CH_4 derived from acetate in acetoclastic methanogenesis (−65‰ to −50‰) (Chanton, 2005; Chanton et al., 2005). Stable isotope ratios can also be useful to detect methanotrophic activity (Conrad, 2005) because CH_4 oxidation by methanotrophic bacteria favors the ^{12}C-isotope, leaving the residual CH_4 enriched in ^{13}C (Whiticar, 1999).

Microbes play a key role in consuming and producing CH_4. They harbor functional genes that encode enzymes involved in CH_4 oxidation (particulate and soluble CH_4 monoxygenases *pmoA* and *mmoX*) and methanogenesis (methyl coenzyme *M* reductase *mcrA*; Dumont & Murrell, 2005; Friedrich, 2005; McDonald & Murrell, 1997). The genetic potential for these processes can be studied by quantifying the abundance of the functional gene copies and by analyzing the community composition of CH_4-related microbes. Usually, a more diverse community performs higher process rates (Graham et al., 2016); however, sometimes molecular data do not reflect contrasting CH_4 emissions (Chaudhary et al., 2017). Evidence linking biogeochemical fluxes and microbial

21698961, 2026, 1, Downloaded from https://agupubs.onlinelibrary.wiley.com/doi/10.1029/2025JG009061 by Readcube (Labtiva Inc.), Wiley Online Library on [19/11/2026]. See the Terms and Conditions (https://onlinelibrary.wiley.com/terms-and-conditions) on Wiley Online Library for rules of use; OA articles are governed by the applicable Creative Commons License

21698961, 2026, 1, Downloaded from https://agupubs.onlinelibrary.wiley.com/doi/10.1029/2025JG009061 by Readcube (Labtiva Inc.), Wiley Online Library on [19/11/2026]. See the Terms and Conditions (https://onlinelibrary.wiley.com/terms-and-conditions) on Wiley Online Library for rules of use; OA articles are governed by the applicable Creative Commons License

diversity is scarce, particularly for CH_4 processes in running waters with most studies performed in rivers with perturbations (reservoirs, urban areas, and agriculture) (Berberich et al., 2020; Burrows et al., 2021; Levine et al., 2011; Mo et al., 2025; Reis et al., 2020; Xing et al., 2023). Furthermore, there is still a lack of knowledge about the ecology and spatial distribution of these microbes within streams, for example, which habitats (sediments, water column, plants) hold higher genetic potential and more diverse communities. Our knowledge of the CH_4-related microbiome in aquatic plants remains notably limited (Ge et al., 2025), particularly in lotic ecosystems. Characterizing the communities across these different habitats and across systems could provide insight as to where methane processes are occurring.

In this study, we investigate the influence of land cover and hydrology on CH_4 and CO_2 emissions from subarctic streams. The main objectives of this study were to (a) quantify the fluxes and stable isotopic signatures of CH_4 and CO_2 emitted from two streams located in catchments dominated by either peatland or upland mineral soil, (b) to assess the influence of seasonal and interannual variation on these fluxes, and (c) to investigate the role of environmental factors (e.g., water discharge, meteorology, DOC, and nutrient availability) and microbial communities (e.g., the *pmoA*, *mmoX* and *mcrA* genetic potential, diversity, and community structure) on stream CH_4 and CO_2 fluxes. We hypothesize that:

1. Fluxes of CH_4 and CO_2 are higher in the peatland dominated catchment due to the higher supply of DOC compared with the upland mineral soil catchment.
2. C sources shift seasonally between terrestrial C inputs from groundwater and surface runoff depending on hydrological conditions and flow state (freshet vs. baseflow conditions).
3. Hydrological conditions and DOC transport into these systems cause seasonal variation in CH_4 and CO_2 fluxes.
4. Within lotic ecosystems, aquatic plants and sediment surfaces are important habitats for CH_4-consuming microbes due to providing fixed structures in an environment with available oxygen and CH_4.

2. Materials and Methods

2.1. Site Description, Sampling, and Measurements

The study was conducted in two subarctic streams in a region located in a coniferous forest in Värriö Strict Nature Reserve in the Finnish Lapland (Figure S1 in Supporting Information S1). The study sites are accessible via the Värriö Subarctic Research station (University of Helsinki, Finland). The dominant tree species in the area include Scots pine (*Pinus sylvestris* L.), Norway spruce (*Picea abies* ssp. *obovata*), and downy birch (*Betula pubescens* ssp. *pubescens*). The soils in the study region are haplic podzols with sand tills (FAO 1990). The climate is subcontinental with no underlying permafrost. The mean annual precipitation and air temperature in the study area are 592 mm (Korhonen & Haavanlammi, 2012) and −1°C (Susiluoto et al., 2008), respectively. The length of the snow cover period is 200–225 days and the length of the growing season 105–120 days (Pohjonen et al., 2008).

Samples were collected from two streams representing contrasting catchment characteristics in terms of vegetation and soil type. Yli-Nuortti, later referred to as a brown-water (BW) stream (67°46′8″ N, 29°12′43″ E, maximum depth of 1.7 m and channel width of 4.5 m), is surrounded by open mires with an approximate peatland coverage in the catchment of 20% and the catchment area of 4,000 ha. The ground vegetation in the catchment consists of dwarf shrubs (*Betula nana* L., *Salix glauca* L.), flowering plants (*Geranium sylvaticum* L.), graminoids, and mosses (*Spaghnum* L.). Kotkakurunoja, a clear-water (CW) stream (67°46′9″ N, 29°40′37″ E, maximum depth of 1.4 m and channel width of 4.0 m), flows through a steep gorge and is surrounded by mineral forest soils with <1% catchment peatland coverage and the catchment area of 1,177 ha. The ground vegetation in the catchment consists of dwarf shrubs (*Vaccinium myrtillus* L., *Vaccinium vitis idaea* L., and *Empetrum nigrum* L.), lichens (*Cladina* (Nyl.)), and mosses (*Polytrichum* sp. and *Pleurozium schreberi* (Brid.) Mitt.).

Sampling and measurements were carried out nine times between June 2022 and October 2023 (see sampling dates in Table S1 in Supporting Information S1). Water samples were collected from the surface water of each stream (~10 cm depth) near the shoreline (Figure S1 in Supporting Information S1) to 50 ml centrifuge tubes (Thermo Scientific™, MA, USA). Water samples were transported immediately to the laboratory and stored in the dark at −18°C until further analysis. The samples were filtered through 0.45 µm syringe filters (Sartorius, CA, USA) before the analyses. Submerged aquatic vegetation and surface sediment samples were collected aseptically

near the shoreline and stored in zip lock polyethene bags at −18°C for further molecular microbiological analysis. The aquatic vegetation in the brown-water stream was dominated by *Hippuris vulgaris* (Figure S2a in Supporting Information S1) and in the clearwater stream by brook moss (*Fontinalis*) (Figure S2b in Supporting Information S1). Data for air temperature, air pressure, and precipitation were obtained from the database of continuous measurements at SMEAR research stations of the University of Helsinki and the University of Eastern Finland (SMEAR I Nuorttiaapa wetland and Värriö forest, available at https://smear.avaa.csc.fi/).

2.2. Water Quality and Nutrient Analyses

Water pH and electric conductivity (EC) were measured with a pH meter (WTW, pH340) and an EC meter (WTW pH/cond 340i), respectively. The concentrations of chloride (Cl^-), sulfate (SO_4^{2-}), phosphate (PO_3^-), nitrate (NO_3^-), and nitrite (NO_2^-) were measured from the water samples filtered through 0.45 µm syringe filters with Ion Chromatography (Dionex ICS-2100, Thermo Scientific).

2.3. DOC and TN Concentration and Optical Analyses

DOC and total nitrogen (TN) concentrations were determined with a standardized method (SFS-EN 1484) using TOC analyzer (Shimadzu TOC-VCPH, Shimadzu Corp., Kyoto, Japan). Spectral absorbance was measured with a laboratory benchtop spectrophotometer (UV-1800, Shimadzu, Kyoto, Japan) between 200 and 800 nm with a 10 mm pathlength quartz cell (acquisition step: 1 nm, scan speed: slow). Wavelength-specific UV-absorbance at 254 nm ($SUVA_{254}$) was calculated as the absorbance divided by the DOC concentration and used as a proxy for DOC aromaticity (Weishaar et al., 2003). Absorption at 350 nm (a_{350}) was converted to Napierian absorbance coefficients (Hu et al., 2002) and used to assess the chromophoric dissolved organic matter (CDOM) content of water samples. Based on these measurements, the ratio of the absorption coefficients at 250 and 365 nm (a_{250}: a_{365}) was calculated, which is inversely related to the aromaticity and molecular weight of DOM (Peuravuori & Pihlaja, 1997).

2.4. Discharge Measurements

Water discharge was determined based on the continuous water depth measurements carried out by pressure sensors measuring the hydrostatic pressure (Levelogger, Solinst, Georgetown, Canada) at the bottom of the river which was corrected by barometric pressure measurements (Barologger, Solinst, Georgetown, Canada). The water depth measurements were converted to discharge using channel cross-section, water depth, and manual discharge measurements (Schiltnecht MiniAir2, Schiltnecht Messtechnik, Switzerland) conducted across the stream at sampling locations.

2.5. Fluxes and Stable Isotopic Analyses of CH_4 and CO_2

Manual floating chamber measurements of CH_4 and CO_2 fluxes were conducted with four to eight replicate chambers at both streams (Bastviken et al., 2010). Chambers were opaque polyethylene plastic buckets with Styrofoam floats and sampling outlets (Gålfalk et al., 2013). Each chamber reached approximately 3 cm into the water, and their height above water was approximately 13 cm. The surface area covered by a chamber was 0.12 m^2 and its headspace was 0.009 m^3. The closing time for the chamber measurements was 21 min, and the gas sampling was conducted 0, 3, 7, 14, and 21 min after the beginning of deployment, except for June 2022, when the closing time was 28 min and sampling interval 7 min. Air samples were taken with 60 ml BD PlastipakTM syringes equipped with a BD Connecta 3-way stopcock valve (Becton, Dickinson and Company, NJ, USA) and injected into pre-evacuated 12 ml Labco Exetainer® vials (Labco Ltd., Lampeter, Ceredigion, UK).

The gas samples collected into Exetainers® were analyzed for the CH_4 and CO_2 concentrations with Agilent 7890B Gas Chromatograph (Agilent Technologies, Palo Alto, CA, USA) equipped with Gilson liquid handler GX271 autosampler (Gilson Inc., Middleton, WI, USA). The CH_4 and CO_2 concentrations versus time were fit using a linear regression. The regression lines with $r^2 > 0.80$ were accepted. For the regression lines with $r^2 < 0.8$, standard error of the regression slope was inspected, and the regression slopes with a high standard error were discarded. As a result, 95% of CH_4 ($n = 99$) and 90% of CO_2 flux ($n = 94$) measurements were accepted. Flux was calculated from the concentration increase in the chamber using equation (Erkkilä et al., 2018):

21698961, 2026, 1, Downloaded from https://agupubs.onlinelibrary.wiley.com/doi/10.1029/2025JG009061 by Readcube (Labtiva Inc.), Wiley Online Library on [19/11/2026]. See the Terms and Conditions (https://onlinelibrary.wiley.com/terms-and-conditions) on Wiley Online Library for rules of use; OA articles are governed by the applicable Creative Commons License

$$F = \frac{dx}{dt}\frac{pV}{RTA} \quad (1)$$

where $\frac{dx}{dt}$ is the slope of the linear fit to concentration increase inside the chamber during the closure time (µl l^{-1} s^{-1}), p ambient pressure (Pa), V the chamber volume (m^3), A the bottom area of the chamber (m^2), R universal gas constant (J mol^{-1} K^{-1}), and T air temperature (K).

A subset of the gas samples was analyzed with Picarro G2201-i isotopic analyzer (Picarro Inc., Santa Clara, CA, USA) equipped with SAM autosampler to determine the stable isotopic values ($\delta^{13}C$) for CH_4 and CO_2. The analyses and corrections applied to the raw data were done as described in detail by Jentzsch et al. (2024). Certified reference gases (2,000 ppm of CO_2 and 10 ppm of CH_4) were also analyzed. Stable isotope values in the reference gases were 41.6 ± 0.5‰ for CH_4 and 34.7 ± 0.3‰ for CO_2. $\delta^{13}C$ values of the emitted CO_2 or CH_4 were calculated with the Keeling plot method (Karlsson et al., 2007). Intercepts with standard error (SE) lower than 3‰ were accepted. 66% (CH_4) ($n = 25$) and 92% (CO_2) ($n = 35$) of the Keeling estimates in the brown-water stream and 56% (CH_4) ($n = 20$) and 64% (CO_2) ($n = 23$) of the Keeling estimates in the clear-water stream were accepted.

2.6. Microbial Molecular Analyses

2.6.1. Molecular Sampling and DNA Extractions

For microbial analyses 18 aquatic plant samples (Figure S2 in Supporting Information S1), 18 water samples, and 12 sediment samples were collected. From water samples, microbial samples were collected into 0.45 µm syringe filters (Sartorius, CA, USA) by filtering until filter saturation; a mean of 220 ml (range 90–584 ml) of water was used (see further details in Table S7 in Supporting Information S1). Note that due to the pore size used, our water sampling protocol targeted mainly microorganisms attached to suspended particles because free microbial cells may have passed the filter. All samples were frozen immediately after sampling, kept frozen during transport, and subsequently stored at −80°C until DNA extraction.

Before DNA extraction, plants were homogenized by grinding in a sterilized mortar and kept frozen using liquid nitrogen. A mean of 0.49 (0.44–0.55) g of plant and of 0.64 (0.33–0.93) g of sediment were extracted for DNA using the DNeasy PowerSoil Pro Kit (Qiagen), following instructions specified by the manufacturer with the following adjustments: (a) cell lysis was achieved by bead-beating in a FastPrep device (Bio 101 FP120-120V, Thermo Fisher Scientific) at 5.5 m s^{-1} for 2 × 30 s. (b) Samples were eluted with 100 µl C6 elution buffer and subsequently centrifuged for 1 min, after which the sample was added a second time to the center of the filter membrane and centrifuged to increase the DNA yield of the sample. Similarly, the DNA from the water filters was extracted using the DNA water kit (Qiagen) and eluted with 30 µl of C6 elution buffer to increase the eluted DNA concentration. DNA quantity and quality were checked with a Qubit® 1.0 Fluorometer (Invitrogen, Thermo Fisher Scientific) using fluorescent dye binding to double-stranded DNA (Qubit) and NanoDrop (ND-1000, Thermo Fisher Scientific) using 260/280 and 260/230 absorbance quality parameters. DNA extracts were stored at −80°C until transported on blue ice to the sequencing laboratory.

2.6.2. Quantitative PCR, Targeted Metagenomics, and Bioinformatics

The molecular analysis focused on the microbes carrying functional genes related to CH_4 cycling, including CH_4 oxidation (*pmoA* (clade 1a, 1b, and type II), *mmoX*) and methanogenesis (*mcrA*). Quantitative real-time PCR (qPCR) was used to quantify *pmoA*, *mmoX*, and bacterial *16S rRNA* gene for the total 48 samples. All qPCR reactions were performed in duplicate in a total reaction volume of 10 µL using GoTaq SYBR Green qPCR kit (Promega), 0.5–1.0 µm of each primer and 5 ng DNA on the Biorad CFX Connect Real-Time System. For some water samples with low DNA content 1 µl of DNA extract instead of 5 ng was loaded. Primers (Kolb et al., 2003; Muyzer et al., 1993; Rahman et al., 2011), amplification protocols and resulting efficiencies for each assay are listed in Table S7 in Supporting Information S1. Potential inhibition of the PCR reactions was checked using three levels of diluted DNA concentration of template; no inhibition of the amplification reactions was detected. Standard curves for each assay were generated by serial dilutions of linearized plasmids with cloned fragments of the respective gene. Standard curves were linear (R^2 = 0.99 ± 0.01, mean ± SD) in the range used, and amplification efficiency was 100% for the 16S rRNA gene and 58%–84% for the functional genes (Table S8 in

21698961, 2026, 1, Downloaded from https://agupubs.onlinelibrary.wiley.com/doi/10.1029/2025JG009061 by Readcube (Labtiva Inc.), Wiley Online Library on [19/11/2026]. See the Terms and Conditions (https://onlinelibrary.wiley.com/terms-and-conditions) on Wiley Online Library for rules of use; OA articles are governed by the applicable Creative Commons License

21698961, 2026, 1, Downloaded from https://agupubs.onlinelibrary.wiley.com/doi/10.1029/2025JG009061 by Readcube (Labtiva Inc.), Wiley Online Library on [19/11/2026]. See the Terms and Conditions (https://onlinelibrary.wiley.com/terms-and-conditions) on Wiley Online Library for rules of use; OA articles are governed by the applicable Creative Commons License

Supporting Information S1). Melting curve profiles were inspected to check for specific amplification. Non-template controls resulted in negligible values.

For year 2022 samples (8 plant, 8 water, and 2 sediment samples), we additionally determined the relative abundance and community composition of organisms involved in CH_4 transformations using a targeted metagenomic tool based on enrichment of the target genes by probe hybridization (Putkinen et al., 2021; Siljanen et al., 2025). Gene specific probes were designed for targeting *pmoA*, *mmoX*, and *mcrA* genes; target probe development and hybridization procedure have been previously described by Siljanen et al. (2025). In brief, probe libraries were designed for the selected marker genes clustered at predefined similarity cut-offs, resulting in >260,000 unique probes, which were further used to selectively enrich target genes in shotgun metagenomic libraries (Siljanen et al., 2025). In a previous case study for the *amoA* gene, this probe capture approach enabled detecting 10 times as many target gene sequences as by traditional metagenomics and resulted in 18%–35% higher alpha diversities compared with PCR amplicon sequencing and traditional metagenomics, respectively (Siljanen et al., 2025). Besides being able to detect a higher diversity in gene sequences, this tool has the potential to capture also rare and novel sequences (Siljanen et al., 2025). Extracted DNA was analyzed via Next-Generation Sequencing (NGS) involving library preparation and Illumina sequencing at the sequencing facility (Arbor Biosciences, NGS Division, Ann Arbor, MI, USA) using the designed probes for hybridization capture. DNA sequencing produced $\sim 5 \times 10^6$ reads per sample and ~58 GB of raw data for the total of 18 samples. Sequence data were analyzed on local supercomputer Puhti (CSC, Espoo, Finland) using bioinformatics pipelines developed in-house. To determine the relative abundances of *mcrA*, *mmoX,* and *pmoA*, a HMMER search (version v3.3.2; Eddy, 2022) was performed using the command *nhmmer* and an *E*-value threshold for inclusion of gene sequences of $E < 0.001$.

Phylogenetic trees were obtained using *nhmmer* output files for the *pmoA* (including *amoA* organisms), *mmoX* (including other similar monoxygenases), and *mcrA* genes. The gene sequences were aligned with reference genes with the MAFFT aligner (Katoh & Standley, 2013). The reference tree for each gene was calculated with an iQ phylogenetic tree on the aligned sequences (Nguyen et al., 2015). The sequencing outcome of each gene was aligned to the reference gene database and the phylogenetic placements were calculated with a maximum-likelihood approach in RAxML (version 8.2.12; A. Stamatakis, 2014). Phylogenetic trees were visualized in iTOL (Letunic & Bork, 2024). Phylogenetic placements for each sample were extracted from *jplace* files using packages *treeio* and *ggtree*, and the community composition was illustrated as bubble plots *ggplot2* package in *R* (version 4.3.1). Gene variants from the same genera were merged for doing these taxonomic bubble plots, which represent the relative abundance for each genus from the total sequence reads of each sample (Figure 4). The sequences are available in the NCBI Sequence Read Archive (PRJNA1261814).

2.7. Statistical Analyses

All statistical analyses were performed using *R* (version 4.3.1, *R* Core Team 2024) in RStudio (RStudio Team 2024). To test for differences between streams and sampling occasions in different variables, Mann-Whitney U test ($n = 2$ groups) or Kruskal-Wallis test with a post-hoc Dunn test ($n > 2$ groups) was applied; these same tests were used for testing differences by groups of samples (e.g., by habitat) in several molecular variables. In all cases, variables were tested for normality using a Shapiro-Wilk test. Correlations between C gas fluxes and other variables were examined using Spearman's rank correlation test. Variables with significant correlations with CH_4 and CO_2 fluxes ($p < 0.05$) were chosen for further analysis.

A Principal Component Analysis (PCA) was performed to visualize relationships between C gas fluxes and environmental variables (FactoMineR package in *R*). Prior to PCA, discharge and DOC flux were standardized to have a zero mean and unit variance. Multiple linear regression analyses were then performed to examine which variables best explain the fluxes of CH_4 and CO_2. All variables were standardized to z-scores to obtain regression coefficients proportional to the influence of each explanatory variable in the models so that their relative importance could be evaluated. Prior to *z*-standardization, all variables were square root transformed to reduce the influence of extreme values, with the exception of precipitation data. To avoid overfitting, the explanatory variables included in the models were selected using the *dredge* function of MuMIn package, and only models in which all variables were significant ($p < 0.05$) were selected. Variables with high (>5.0) variance inflation factors (VIF) were excluded from the models to remove multicollinearity. Best fitting models were selected based on Akaike's information criterion (AICc) and R^2 determined by the *anova* function of the package stats. Furthermore,

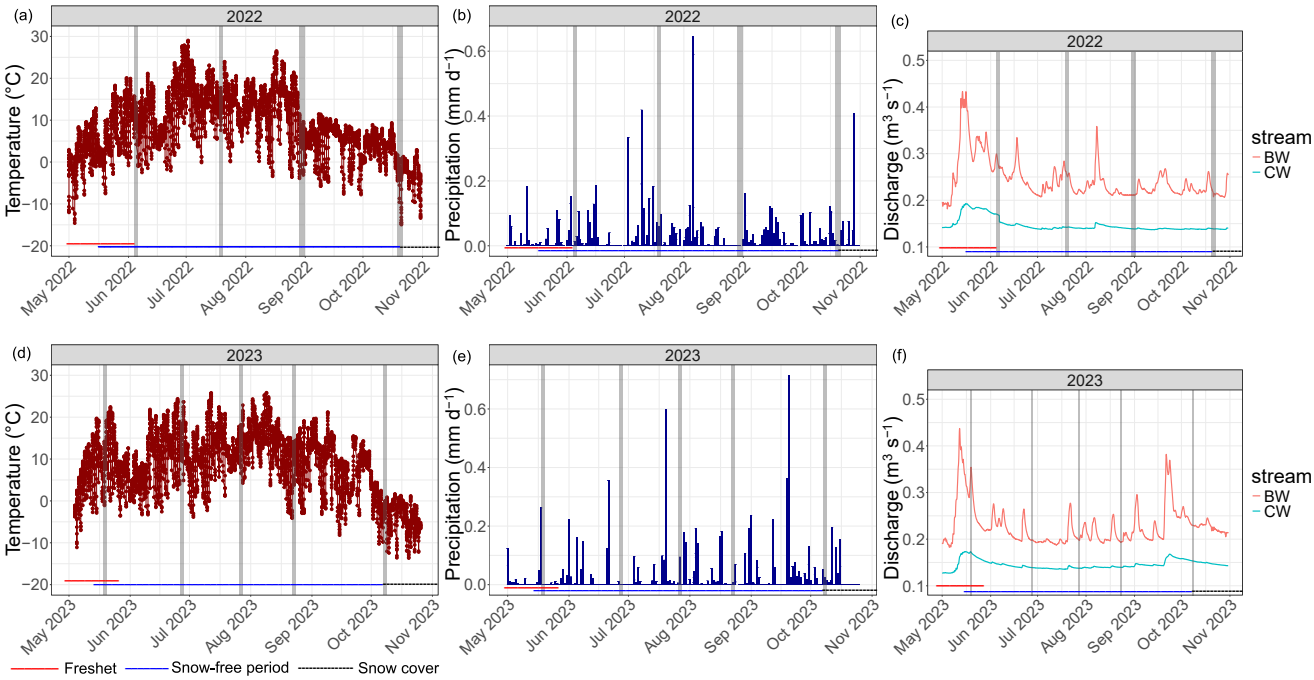


Figure 1. Air temperature (°C) in (a) 2022 and (d) 2023, precipitation (mm d^{-1}) in (b) 2022 and (e) 2023, and water discharge (m^3 s^{-1}) in the brown-water (BW) and clear-water (CW) stream in (c) 2022 and (f) 2023. Gray shaded areas indicate the sampling occasions.

alternative mixed regression models were developed using catchment and sampling occasion as random factors to account for unquantified catchment- or time-specific variation. Regression models were fitted with the *lm* function of the *R* core package stats and mixed models with the *lme* function of the package *nlme*. For comparison of regression and mixed models using the *anova* function, regression models were fitted with the *gls* function of the package *nlme*.

PCA using Hellinger distance (Legendre & Gallagher, 2001) was performed to see the ordinations of the gene variants of the microbes carrying functional genes related to CH_4 cycling; particularly to identify the gene variants with a significant influence in the principal components (PC). Using the *envfit* function of the Vegan package we identify the variables significantly correlated to the PC which were added to the PCA plots (Figures S6–S8, Tables S9–S11 in Supporting Information S1). Using all nodes of the phylogenetic placements files (jplace) for each functional gene the diversity index (Shannon-Weiner), the gene variant (node) richness, as well as the alpha-, beta-, and gamma-diversities were calculated using *R* package *vegan* (Tables S2 and S3 in Supporting Information S1).

3. Results

3.1. Weather Conditions and Annual Discharge

The year 2023 (the annual mean of −0.4°C) was colder compared with the year 2022 (the annual mean of 0.2°C; $p < 0.001$) (Figures 1a and 1d). Both years were warmer compared with the 30-year annual mean of −1°C (Pirinen et al., 2012). The annual precipitation was similar in both years (598 and 578 mm in 2022 and 2023, respectively; $p = 0.69$) (Figures 1b and 1e), and close to the long-term mean annual precipitation of 592 mm (Pirinen et al., 2012).

In both streams, discharge (Q) was strongly seasonal with the highest Q detected during spring freshet in May and lowest Q during baseflow in the winter (Figures 1c and 1f). Q varied from 0.16 to 0.44 m^3 s^{-1} in the brown-water (BW) stream and from 0.13 to 0.19 m^3 s^{-1} in the clear-water (CW) stream, being significantly higher in the BW stream ($p < 0.001$). In the BW stream, Q was higher in 2022 compared with 2023 ($p < 0.001$) and responded to variation in precipitation.

21698961, 2026, 1, Downloaded from https://agupubs.onlinelibrary.wiley.com/doi/10.1029/2025JG009061 by Readcube (Labtiva Inc.), Wiley Online Library on [19/11/2026]. See the Terms and Conditions (https://onlinelibrary.wiley.com/terms-and-conditions) on Wiley Online Library for rules of use; OA articles are governed by the applicable Creative Commons License

3.2. Fluxes of DOC, CH_4, and CO_2

The flux of DOC exported from the BW stream was higher compared with the flux exported from the CW stream ($p < 0.001$) (Figure 2b). The DOC fluxes normalized to catchment area ranged from 0.6 to 10.3 mg C m^{-2} d^{-1} in the BW stream (median 3.5 mg C m^{-2} d^{-1}) and from 0.1 to 0.5 mg C m^{-2} d^{-1} in the CW stream (0.3 mg C m^{-2} d^{-1}), with the maximum DOC fluxes occurring during the spring freshet in May 2023 (Figure 2b).

The CH_4 fluxes were on average higher in the BW stream compared with the CW stream ($p < 0.001$), varying from 2.0 to 68.1 mg C m^{-2} d^{-1} in the BW stream (median 7.8 mg C m^{-2} d^{-1}) and from 1.6 to 7.3 mg C m^{-2} d^{-1} in the CW stream (3.9 mg C m^{-2} d^{-1}) (Figure 2e). The CH_4 fluxes varied between sampling occasions ($p < 0.001$). In the BW stream, the highest CH_4 fluxes were generally detected during spring or early summer, after which the fluxes decreased toward autumn. However, in the CW stream, the highest CH_4 fluxes were detected during late summer (July–August) in both years. While the CH_4 fluxes in the BW stream were similar between the years, the CH_4 fluxes in the CW stream were on average higher in 2022 (median 5.6 mg C m^{-2} d^{-1}) compared with the year 2023 (3.4 mg C m^{-2} d^{-1}) ($p = 0.02$).

As for the CH_4 fluxes, also the CO_2 fluxes were higher in the BW stream compared with the CW stream ($p < 0.001$) (Figure 2f). The CO_2 fluxes ranged from 242.0 to 2293.0 mg C m^{-2} d^{-1} in the BW stream (median 802.6 mg C m^{-2} d^{-1}) and from 46.2 to 921.0 mg C m^{-2} d^{-1} in the CW stream (220.9 mg C m^{-2} d^{-1}). The CO_2 fluxes were significantly different between the sampling occasions ($p < 0.001$), with the highest CO_2 fluxes in both streams generally measured during spring (May–June). No significant differences in the CO_2 fluxes occurred between the years.

3.3. Water Quality and Optical Properties of DOM

pH and electrical conductivity (EC) were similar in both streams (Table 1). Sulfate (SO_4^{2-}) was the dominant anion in both the BW and CW streams (Table 1). The concentrations of nitrate (NO_3^-) were very low and similar in both streams (Table 1). Furthermore, in both streams, the concentrations of Cl and NO_3^- were higher in 2022 than in 2023 ($p < 0.001$) (Figure S3a and S3b in Supporting Information S1).

DOC concentrations were higher in the BW stream compared with the CW stream ($p < 0.001$) (Table 1). The BW stream also had higher TN concentrations compared with the CW stream ($p = 0.002$) (Table 1). Both DOC ($p = 0.003$) and TN ($p = 0.02$) concentrations varied between the sampling occasions, being highest in the early summer or mid-summer (Figures S3d and S3e in Supporting Information S1). In the CW stream, DOC concentrations were higher in 2023 than in 2022 ($p < 0.001$) (Figure S3d in Supporting Information S1).

While $SUVA_{254}$ values did not significantly differ between the two streams (Table 1), the ratio between the absorbance at 250 and 365 nm (a_{250}:a_{365}) as well as CDOM absorbance (a_{350}) were different between the BW and CW streams ($p = 0.003$ and $p = 0.005$, respectively) (Table 1). There were no clear seasonal differences in the optical parameters of DOM. In both streams, $SUVA_{254}$ was higher in 2022 compared with 2023 ($p < 0.001$) (Figure S3h in Supporting Information S1). In the CW stream, a_{250}:a_{365} was higher and a_{350} lower in 2022 compared with 2023 ($p < 0.001$) (Figures S3f and S3g in Supporting Information S1).

3.4. Stable Isotopic Composition of C in CH_4 and CO_2

The $\delta^{13}C$ values of emitted CH_4 were lower in the CW stream compared to the BW stream ($p = 0.02$, Table 1, Figure 3a). In the BW stream, the $\delta^{13}C$-CH_4 values varied between seasons ($p = 0.02$), shifting toward a more depleted $\delta^{13}C$-CH_4 signature in the autumn (-63 ± 1‰ in October 2022 and -61 ± 6‰ in October 2023). In the CW stream, the $\delta^{13}C$-CH_4 values increased from July–October 2023 ($p = 0.02$) while there were no clear seasonal differences in the $\delta^{13}C$-CH_4 values during 2022.

The $\delta^{13}C$ values of CO_2 fluxes varied from -35 to -22‰ in the BW stream and from -37 to -22 ‰ in the CW stream, being higher in the BW stream ($p = 0.03$, Table 1, Figure 3b). Generally, the $\delta^{13}C$-CO_2 values were more enriched in spring compared to summer and autumn. In 2022, the $\delta^{13}C$-CO_2 values of the BW stream were higher in June (-26 ± 1‰) than in August (-32 ± 2 ‰) or October (-30 ± 1‰) ($p = 0.001$ and $p = 0.03$, respectively). In 2023, the highest $\delta^{13}C$-CO_2 values of the BW stream were detected in May (-23 ± 1‰, $p < 0.001$), followed by a notable decrease in the $\delta^{13}C$-CO_2 values in June (-31 ± 2‰, $p < 0.001$). In the CW stream, the highest $\delta^{13}C$-CO_2 values were also detected during May 2023 (-25 ± 3‰, $p < 0.001$). However, in the CW stream, $\delta^{13}C$-CO_2

21698961, 2026, 1, Downloaded from https://agupubs.onlinelibrary.wiley.com/doi/10.1029/2025JG009061 by Readcube (Labtiva Inc.), Wiley Online Library on [19/11/2026]. See the Terms and Conditions (https://onlinelibrary.wiley.com/terms-and-conditions) on Wiley Online Library for rules of use; OA articles are governed by the applicable Creative Commons License

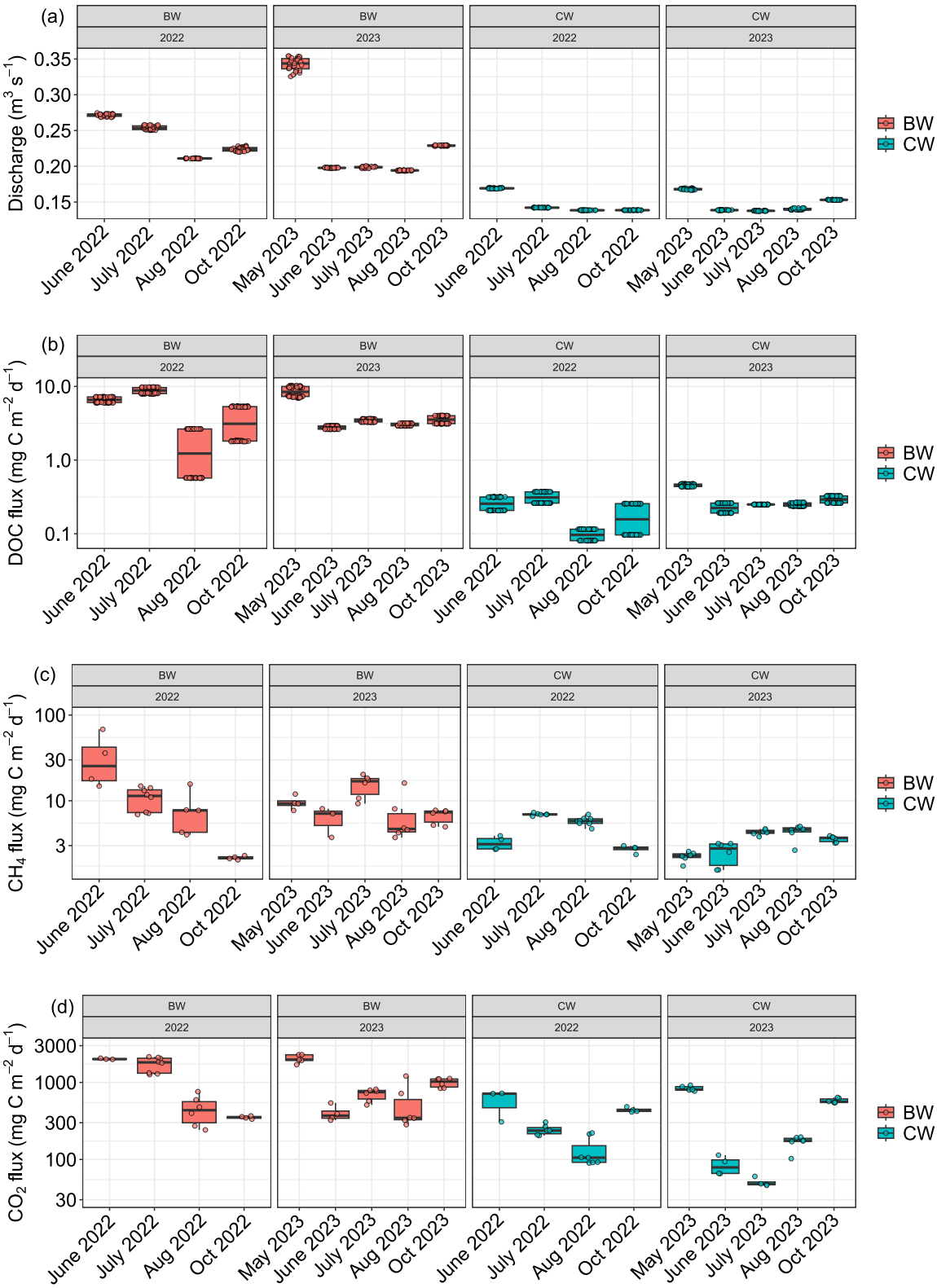


Figure 2. (a) Daily mean discharge ($m^3\ s^{-1}$) and (b) daily mean DOC flux normalized to catchment area (mg C $m^{-2}\ d^{-1}$) during the sampling days; (c) CH_4 flux (mg C $m^{-2}\ d^{-1}$) and (d) CO_2 flux (mg C $m^{-2}\ d^{-1}$) from the brown-water (BW) and clear-water stream (CW) measured with manual floating chambers in 2022 and 2023 (n = 4–8). Boxes are bound by 25th and 75th percentiles, whiskers show 1.5 interquartile range. Solid line represents median values while the dots show the outliers. Positive values indicate outward flux from the waterbodies into the atmosphere.

21698961, 2026, 1, Downloaded from https://agupubs.onlinelibrary.wiley.com/doi/10.1029/2025JG009061 by Readcube (Labtiva Inc.), Wiley Online Library on [19/11/2026]. See the Terms and Conditions (https://onlinelibrary.wiley.com/terms-and-conditions) on Wiley Online Library for rules of use; OA articles are governed by the applicable Creative Commons License

21698961, 2026, 1, Downloaded from https://agupubs.onlinelibrary.wiley.com/doi/10.1029/2025JG009061 by Readcube (Labtiva Inc.), Wiley Online Library on [19/11/2026]. See the Terms and Conditions (https://onlinelibrary.wiley.com/terms-and-conditions) on Wiley Online Library for rules of use; OA articles are governed by the applicable Creative Commons License

Table 1
pH, Electric Conductivity, the Concentrations of Sulfate (SO_4^{2-}), Nitrate (NO_3^-), Chloride (Cl^-), Dissolved Organic Carbon (DOC) and Total Nitrogen (TN), Specific Ultraviolet Absorbance at 254 nm ($SUVA_{254}$), the Ratio Between the Absorbance at 250 and 365 nm (a_{250}:a_{365}), Chromophoric DOM (CDOM) Absorbance at 350 nm (a_{350}), and the $\delta^{13}C$ Values for CH_4 and CO_2 in the Brown-Water (BW) and Clear-Water (CW) Stream During the Measuring Campaigns in 2022 and 2023. n = 9, Except for $\delta^{13}C$-CH_4 and $\delta^{13}C$-CO_2, n = 25 and 35 in the BW Stream and n = 20 and 23 in the CW Stream, Respectively

	BW stream	CW stream
	mean ± sd	mean ± sd
pH	6.7 ± 0.5	7.1 ± 0.6
EC (µS cm^{-1})	29 ± 14	32 ± 9
SO_4^{2-} (mg l^{-1})	1.9 ± 0.5	2.3 ± 0.5
NO_3^- (mg l^{-1})	0.1 ± 0.0	0.1 ± 0.0
Cl^- (mg l^{-1})	1.0 ± 0.4	0.8 ± 0.2
DOC (mg l^{-1})	8.8 ± 3.5	4.7 ± 1.4
TN (mg l^{-1})	0.5 ± 0.2	0.2 ± 0.2
$SUVA_{254}$ (l mg^{-1} m^{-1})	2.7 ± 0.3	2.3 ± 0.6
a_{250}:a_{365}	5.1 ± 1.0	7.8 ± 2.7
a_{350} (m^{-1})	18.4 ± 7.2	8.9 ± 5.1
$\delta^{13}C$-CH_4	−59 ± 4‰	−62 ± 4‰
$\delta^{13}C$-CO_2	−29 ± 3‰	−31 ± 5 ‰

estimates from five sampling occasions had to be discarded due to low accuracy of the Keeling estimates related to low flux rates.

3.5. Abundance and Community Composition of Microbes Harboring CH_4-Related Functional Genes

The number of gene copies of microbes (16S rRNA) and functional genes related to methanotrophy (*mmoX* and *pmoA*) did not significantly differ between the streams and seasons (Figure S4, Table S7 in Supporting Information S1). Also, richness and Shannon diversity of methanotrophs (*pmoA* and *mmoX*) and methanogens (*mcrA*) detected in the aquatic plant and sediment samples showed no significant differences between streams (Figure 4, Table S2 in Supporting Information S1). However, the number of *pmoA* gene copies quantified from submerged aquatic plants was higher in the CW stream compared with the BW stream ($p = 0.01$, Figure 4a, Figure S4d in Supporting Information S1). The amount of DNA and the number of gene copies of microbes (16*S* rRNA) and methanotrophs (*pmoA* and *mmoX*) differed between habitats being several orders of magnitude higher in submerged aquatic plants and surficial sediments than in water particles ($p < 0.001$, Table S7 in Supporting Information S1). Furthermore, diversity of methanotrophs was higher in plant and sediment than in water, that is, Shannon diversity and richness of *pmoA* and *mmoX* genes ($p < 0.05$, except for *pmoA* diversity, Figure 4, Table S3 in Supporting Information S1). For all habitats, the number of *pmoA* copies was higher than *mmoX* copies ($p = 0.001$, Table S7 in Supporting Information S1). Also, the number of *pmoA* reads was higher than *mcrA* reads ($p < 0.001$, Table S2 in Supporting Information S1).

CH_4 and CO_2 fluxes were correlated with several microbial molecular variables. These correlations were stronger with the data divided by stream (Tables S12 and S13 in Supporting Information S1). In the BW stream, the CH_4 flux was positively correlated with the plant *pmoA* copies, *mcrA* richness and diversity, and with the sediment 16S rRNA, *pmoA*, and *mmoX* copies, while it was negatively correlated only with the plant *mmoX* diversity. In the CW stream, the CH_4 flux correlated positively with the plant *pmoA* copies and richness and with the water *mmoX* copies, and negatively with the water 16S rRNA copies, *pmoA* copies, and *mmoX* richness and diversity.

Regarding the methanotrophs, the communities of the microbes harboring *pmoA* gene were diverse, with habitat and time distinguishing the community rather than the stream ($p < 0.05$, Figure 4a, Figure S6, Table S9 in Supporting Information S1). The communities in plant and sediment were more diverse and different from water, particularly in June when *Methylobacter* was abundant and there were higher CH_4 and CO_2 fluxes, $\delta^{13}C$-CO_2 values, discharge, and CH_4-related microbes (i.e., higher *pmoA* copies, *mmoX* copies and reads, and *mcrA* reads, Fig. S6 in Supporting Information S1). Toward fall the communities became more similar between the habitats, with *Methyloglobulus* being the most abundant genera in all habitats and months except for June. Communities of *mmoX* differed by stream ($p = 0.001$, Figure 4b, Figure S7, Table S10 in Supporting Information S1). Genus *Methylovulum* and *Methylomonas* were more abundant in the BW stream while the genera *Bradyrhizobium* dominated in the CW stream. Communities of methanogens (m*crA*) mainly differed by month and habitat ($p < 0.05$, Figure 4c, Figure S8, Table S11 in Supporting Information S1). In June, *mcrA*-harboring microbes were found in all the habitats while they were absent from water samples for the rest of the growing season and found only in half of the plant samples in August and October. In June, the *mcrA* community was more diverse with genus *Methanoregula*, *Methanomassiliicoccus*, and *Methanosaeta* being abundant, while in the following months the communities got simpler, reaching the extreme of harboring only the genera *Methanobacterium*, which is the overall most abundant genus, and from that genus only single species *M. lacus*.

3.6. Relationships Between C Gas Fluxes and Environmental Variables

Principal component analysis (PCA) was conducted to investigate patterns in seasonality and environmental variables for each sample (Figure 5, Figure S6, Table S5 in Supporting Information S1). PC1 explained 41% of the

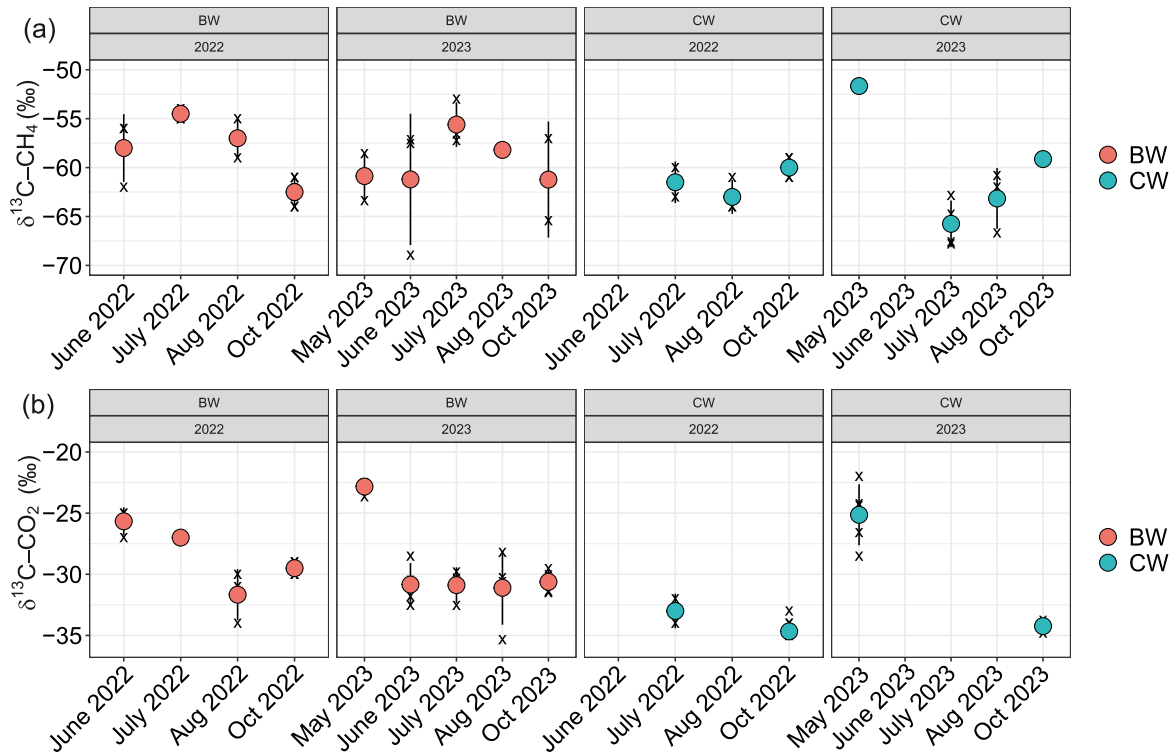


Figure 3. The $\delta^{13}C$ values for (a) CH_4 and (b) CO_2 in the brown-water (BW) and clear-water (CW) stream measured with manual floating chambers in 2022 and 2023 (n = 1–5). Average value (red/blue points) ± standard deviation as well as the individual observations (black crosses) are reported.

variance while PC2 explained 21% of the variance. PC1 was driven negatively by sulfate (SO_4^{2-}) concentration and pH, and positively by CO_2 flux, DOC concentration, and $\delta^{13}C$-CO_2. PC2 was driven negatively by the number of *16S rRNA* gene copies of water particles, and positively by gene variant richness of *mmoX* and *mcrA* from aquatic plant samples.

Environmental variables influencing CH_4 and CO_2 fluxes were further assessed with multiple linear regression models (Table 2, Table S6 in Supporting Information S1). Results from the multiple linear regression analysis showed that water discharge, precipitation, and the quantity of DOC were the most important factors predicting the variation in the C gas fluxes. Model 1b explained 61% of the variance in the CH_4 fluxes ($p < 0.001$). Model 1b showed a significant positive relationship for the CH_4 fluxes with DOC fluxes and precipitation and included the sampling occasion as a random factor. In addition, species richness (S) of methanotrophs (*mmoX*) and the Shannon diversity (H) of methanogens (*mcrA*) in the aquatic plants were positively related to CH_4 fluxes, explaining 45% of the variance in the CH_4 fluxes ($p < 0.001$; model 10). Model 6b explained 91% of the variation in the CO_2 fluxes ($p < 0.001$). Model 6b showed the CO_2 fluxes to have a significant positive relationship with water discharge, DOC concentration, and precipitation, including the sampling occasion as a random factor.

4. Discussion

4.1. Landscape Control on C Gas Emissions From Subarctic Streams

Two-year measurements of C gas fluxes in two pristine subarctic streams draining contrasting catchments showed that the streams acted as sources of CH_4 and CO_2 from spring to late autumn. The fluxes of CO_2 from the BW and CW streams (mean 1026 ± 674 and 335 ± 262 mg C m^{-2} d^{-1}, respectively) were lower than those measured in Siberian (2400 ± 2570 mg C m^{-2} d^{-1}; Krickov et al., 2023) and northern Sweden streams (15,600 ± 8,000 mg C m^{-2} d^{-1}; Lundin et al., 2013), but similar to those in the Upper and Middle Yukon River basin (72 and 744 mg C m^{-2} d^{-1}, respectively; Striegl et al., 2012). Furthermore, the fluxes of CH_4 (11 ± 11 and 4 ± 2 mg C m^{-2} d^{-1} from the BW and CW streams, respectively) were similar or even higher than those in the Yukon River (mean 1 mg C m^{-2} d^{-1} in the Upper and 5 mg C m^{-2} d^{-1} in the Middle Yukon River Basin; Striegl

21698961, 2026, 1, Downloaded from https://agupubs.onlinelibrary.wiley.com/doi/10.1029/2025JG009061 by Readcube (Labtiva Inc.), Wiley Online Library on [19/11/2026]. See the Terms and Conditions (https://onlinelibrary.wiley.com/terms-and-conditions) on Wiley Online Library for rules of use; OA articles are governed by the applicable Creative Commons License

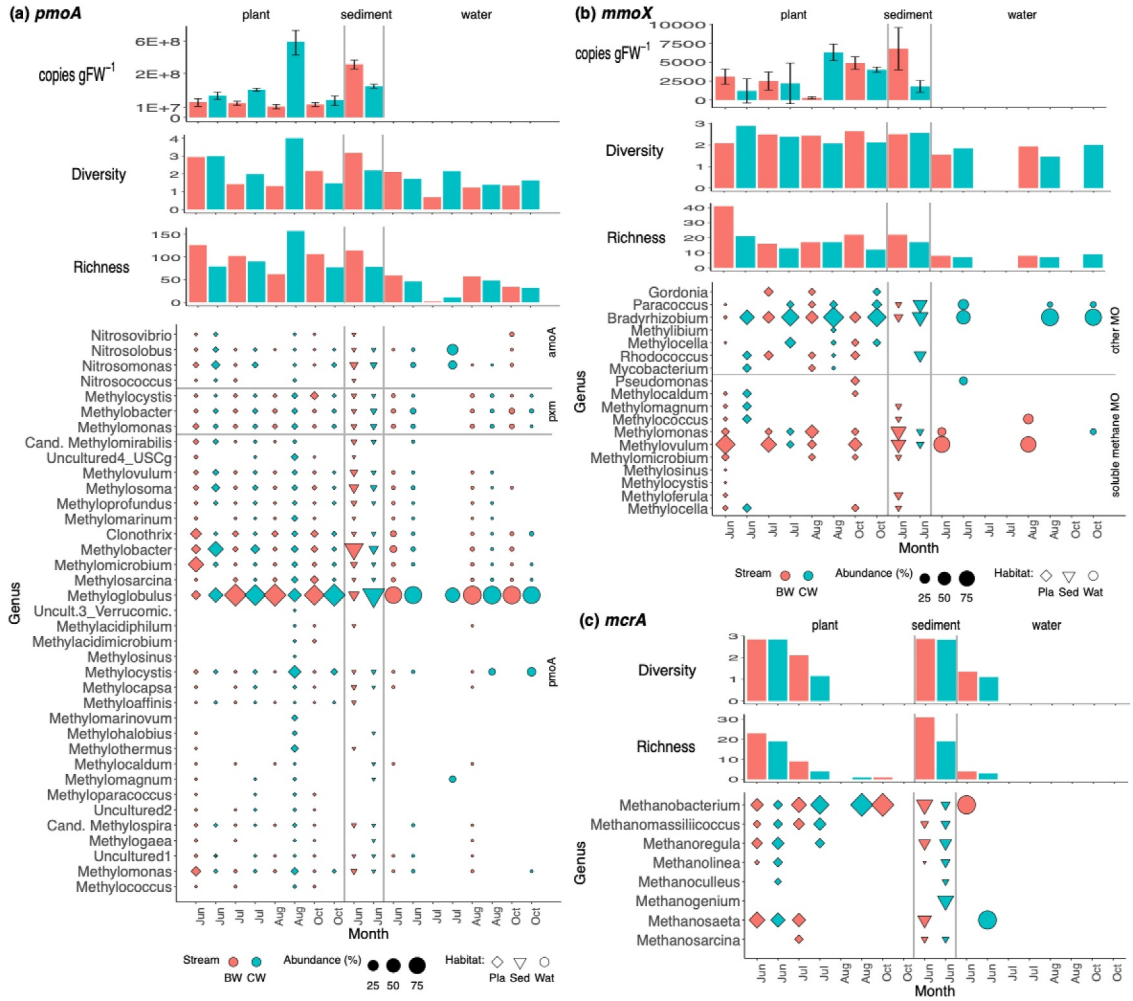


Figure 4. Abundance and community composition of microbes harboring CH_4-related functional genes–(a) *pmoA*, (b) *mmoX*, and (c) *mcrA*–from the brown-water (BW) and clear-water (CW) stream in submerged aquatic plants, surficial sediments, and water particles in 2022. For each gene, the top bar-plot shows the gene abundance (copies gFW^{-1}, average value ± standard deviation, $n = 2$, NA for *mcrA*) while the middle and bottom bar-plots show the Shannon diversity and the richness of the gene variants, respectively. The bubble-plot shows the relative abundance (%) of the Genus harboring each gene variant.

et al., 2012), but lower than in a subarctic catchment in Abisko, northern Sweden (190 ± 30 mg C m^{-2} d^{-1}; Lundin et al., 2013). This demonstrates high variability in regional C gas emission estimates of catchments across strongly heterogeneous northern landscapes, where the relative importance of CH_4 and CO_2 sources (e.g., surface flow, groundwater, carbonate equilibrium processes, and in-stream microbial processing of OC; Striegl et al., 2012) varies depending on land cover characteristics.

The BW stream draining through pristine mire catchment was associated with higher CH_4 and CO_2 fluxes compared with the CW stream surrounded by mineral upland catchment. The positive relationships between the C gas fluxes and DOC quantity (Table 2) suggest that the lateral transport of terrestrial DOC had a crucial role in regulating CH_4 and CO_2 fluxes from subarctic streams, and that the differences in the CH_4 and CO_2 fluxes were driven by the differences in catchment characteristics (e.g., land cover, soil type, and vegetation). In addition to higher concentrations and export of DOC, the BW stream exhibited DOM with higher molecular weight (indicated by the lower a_{250}:a_{365} values) and higher plant-derived chromophoric DOM content (a_{350}). Since increases in a_{350} have been previously linked to higher catchment vegetation cover (Johnston et al., 2021), the observed positive relationships between C gas fluxes, DOC quantity and CDOM content suggest that the increasing vegetation cover due to climate change (greening; Finstad et al., 2016) could increase the release of CH_4 and CO_2 from streams to the atmosphere. While streams draining mineral soil catchments tend to export a larger proportion of biolabile molecular compounds (Johnston et al., 2021), the concentrations of DOC in mineral soil catchment

21698961, 2026, 1, Downloaded from https://agupubs.onlinelibrary.wiley.com/doi/10.1029/2025JG009061 by Readcube (Labtiva Inc.), Wiley Online Library on [19/11/2026]. See the Terms and Conditions (https://onlinelibrary.wiley.com/terms-and-conditions) on Wiley Online Library for rules of use; OA articles are governed by the applicable Creative Commons License

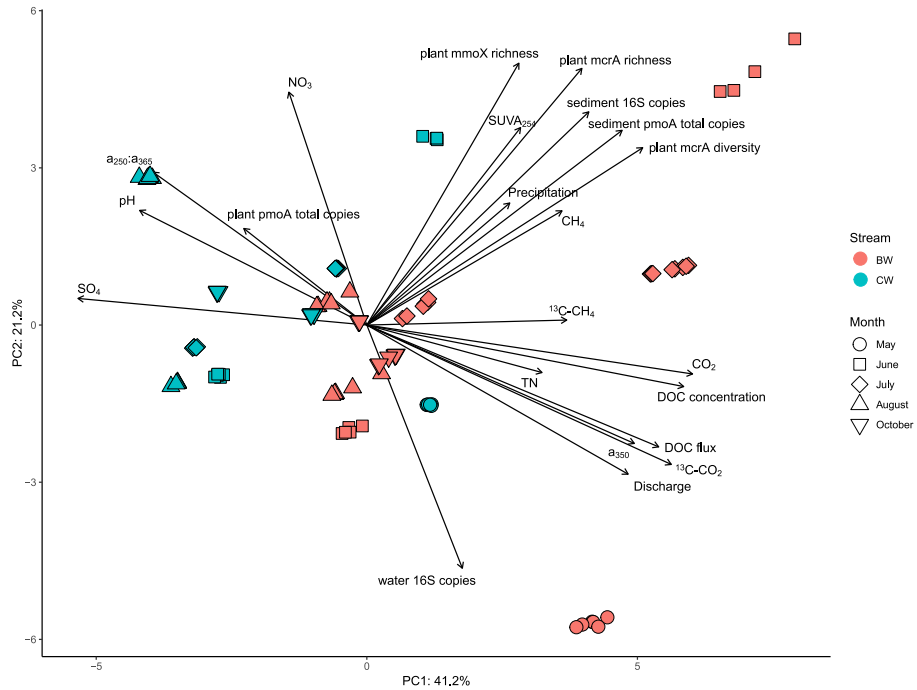


Figure 5. Principle component analysis (PCA) of CH_4 and CO_2 fluxes and environmental variables in the brown-water (BW) and clear-water stream (CW). Each point in the PCA represents a sampling event. Points are colored by stream and shaped by month. Prior to analysis, discharge and DOC flux were standardized to have a zero mean and unit variance. $n = 103$.

were clearly lower compared with the DOC concentrations in mire dominated catchment. Therefore, despite the higher degradation potential of DOC in the CW stream draining through upland mineral soil catchment (Saarela et al., 2024), the results here support our first hypothesis that the higher export of DOC from peatlands results in higher emissions of CO_2 and CH_4 from streams to the atmosphere.

Humic colored DOM compounds detected in the BW stream, as indicated by a_{350}, are highly sensitive to photodegradation, which can further generate products stimulating aquatic bacterial metabolism and CO_2 release (Cory et al., 2013). Both photochemical and biological degradation of DOM have also been attributed to the supply and interactions with nutrients (Berggren et al., 2022; Guillemette et al., 2013). The fluxes of CH_4 showed a negative relationship with the concentrations of SO_4^{2-} (Table S4 in Supporting Information S1). This relationship was also seen as the lower SO_4^{2-} concentrations coinciding with the higher CH_4 fluxes in the BW stream compared with the CW stream. This is consistent with earlier studies showing that the peatland percentage in the catchment may not be a good predictor for stream water SO_4^{2-} concentrations, although peatlands and their riparian zones can influence the biogeochemistry and transformation processes of SO_4^{2-} (e.g., dissimilatory

Table 2
Results of Multilinear Regression Analysis for Predicting CH_4 flux (Models 1a–b and 10) and CO_2 Flux (Models 6a–b) From Environmental Variables

Model	Formula: Fixed//random	AICc	R^2
1a	$\sqrt{CH_4} = 0.43 \times \sqrt{DOC_{FLUX}} + 0.28 \times$ Precipitation	222	0.34
1b	$\sqrt{CH_4} = 0.48 \times \sqrt{DOC_{FLUX}} + 0.32 \times$ Precipitation//random = ~1|month	211	0.61
10	$\sqrt{CH_4} = 0.50 \times \sqrt{\text{Plant mmoX S}} + 0.35 \times \sqrt{\text{Plant mcrA H}}$	95.6	0.45
6a	$\sqrt{CO_2} = 0.60 \times \sqrt{\text{Discharge}} + 0.36 \times \sqrt{DOC_{CONC}} + 0.14 \times$ Precipitation	102	0.83
6b	$\sqrt{CO_2} = 0.62 \times \sqrt{DOC_{CONC}} + 0.32 \times$ Precipitation $+ 0.28 \times \sqrt{\text{Discharge}}$//random = ~1|month	96	0.91

Note. Only models with all explanatory variables significant ($p < 0.05$) are presented. For all variables, variance inflation factor (VIF) was <5. "Month" refers to the sampling occasion used as a random factor in linear mixed-effects models. "*Plant mmoX S*" refers to species richness of *mmoX* genes and "*plant mcrA H*" to Shannon diversity of *mcrA* genes in the aquatic plant samples. R^2 refers to adjusted R^2. $n = 89$ in models 1a–b and 6a–b, $n = 40$ in model 10.

21698961, 2026, 1, Downloaded from https://agupubs.onlinelibrary.wiley.com/doi/10.1029/2025JG009061 by Readcube (Labtiva Inc.), Wiley Online Library on [19/11/2026]. See the Terms and Conditions (https://onlinelibrary.wiley.com/terms-and-conditions) on Wiley Online Library for rules of use; OA articles are governed by the applicable Creative Commons License

sulfate reduction; Mörth et al., 2008). Furthermore, the negative relationship between CH_4 flux and SO_4^{2-} concentration might suggest that oxygen-limited conditions favoring methanogenesis were also favorable for SO_4^{2-} reducing bacteria in stream sediments (Kuivila et al., 1989). In anoxic sediments, methanogenesis might be inhibited by the high availability of SO_4^{2-} because sulfate-reducing bacteria outcompete methanogens for substrate uptake of H_2 and acetate (Winfrey & Zeikus, 1977).

The δ^{13}C-CH_4 values were significantly higher in the BW stream compared with the CW stream. First, such variation in the measured δ^{13}C-CH_4 values between the two streams might be due to differences in dominant methanogenic pathways, that is, acetoclastic (−65 to −50‰) versus hydrogenotrophic methanogenesis (−100 to −60‰) (Chanton, 2005; Chanton et al., 2005). Second, the higher δ^{13}C-CH_4 values detected in the BW stream during mid-summer could be indicative of aerobic CH_4 oxidation, because methanotrophic activity leaves the residual CH_4 enriched in ^{13}C, resulting in higher δ^{13}C-CH_4 values (Coleman & Raiswell, 1981). Since the availability of CH_4 is a key factor that determines its oxidation rates in aquatic environments (Duc et al., 2010; Sepulveda-Jauregui et al., 2018), the relatively high CH_4 fluxes measured during July could indicate sufficient CH_4 availability supporting CH_4 oxidation in the BW stream. The positive relationship between CH_4 flux and the number of particulate CH_4 monooxygenase *pmoA* gene copies in the sediment samples (Table S4 in Supporting Information S1, Figure 4), used as a biomarker for the abundance of methanotrophs (McDonald & Murrell, 1997), further implies that the increased CH_4 availability enabled methanotrophic activity in the sediment of the BW stream.

Similarly to δ^{13}C-CH_4, the stable isotopic values of δ^{13}C-CO_2 were higher in the BW stream compared with the CW stream. Previously, more positive δ^{13}C-DIC values coinciding with high CO_2 concentrations have been detected in catchments with the largest proportion of peatlands (Campeau et al., 2017). Peatlands export large quantities of C gases to streams (Dinsmore et al., 2010), and they are fueled by anaerobic processes that can notably alter δ^{13}C signatures (Waldron et al., 1999; Whiticar et al., 1986). On the other hand, the more enriched δ^{13}C-CO_2 in the BW stream could also imply CO_2 production from more decomposed C sources (Dorrepaal et al., 2009) because more decomposed C tends to be enriched in ^{13}C due to selective loss of ^{12}C (Natelhoffer & Fry, 1988; Ågren et al., 1996). This is also supported by the relationships between δ^{13}C-CO_2 signatures and DOM optical parameters (e.g., a_{250}:a_{365} and a_{350}, Table S4 in Supporting Information S1), indicating higher δ^{13}C-CO_2 values with more recalcitrant DOM.

These findings suggest a dominant role of land cover in regulating the fluxes of CH_4 and CO_2 from subarctic streams. While a variety of studies have reported decreased bioavailability of stream water DOM in catchments containing a higher proportion of peatland land cover (Berggren et al., 2007; Fellman et al., 2008; Saarela et al., 2024), our findings indicate that high loads of DOM are associated with significantly higher stream C gas release from peatland dominated catchment compared to upland mineral soil catchment, regardless of the intrinsic properties and quality of DOM.

4.2. In-Stream Processing of OC

In low order streams, soil respiration is often considered the main source of inorganic C gases, rather than in-stream processing (Dawson et al., 2001). However, since CO_2 in streams becomes isotopically lighter (i.e., more negative δ^{13}C values) due to internal processes (e.g., autochthonous primary production and DOC mineralization), the more negative stable isotopic composition of CO_2 in the CW stream compared with the BW stream could indicate the occurrence of in-stream processing (Campeau et al., 2017). The most depleted ^{13}C values of CO_2 in the CW stream are similar to those reported for δ^{13}C of autochthonous sources (−47.0‰ to −35.7‰) from unproductive Scandinavian lakes (Karlsson et al., 2007, and references therein). These results suggest that while the CO_2 emitted from the BW stream predominantly originated from terrestrial peatland sources, the CO_2 from the CW stream could be additionally fueled by in-stream primary productivity. The role of autochthonous sources could be important in the CW stream particularly during baseflow periods because the presence of autochthonous production in fluvial networks is often linked to longer residence times and lower water discharge (Roach et al., 2014). Indeed, the CW stream was associated with significantly lower water discharge and four times smaller catchment size compared to the BW stream. On the other hand, the more negative δ^{13}C values of the emitted CO_2 in the CW stream compared with the BW stream could also be due to the CO_2 derived from CH_4 oxidation in the stream or soil waters (Barker & Fritz, 1981).

21698961, 2026, 1, Downloaded from https://agupubs.onlinelibrary.wiley.com/doi/10.1029/2025JG009061 by Readcube (Labtiva Inc.), Wiley Online Library on [19/11/2026]. See the Terms and Conditions (https://onlinelibrary.wiley.com/terms-and-conditions) on Wiley Online Library for rules of use; OA articles are governed by the applicable Creative Commons License

21698961, 2026, 1, Downloaded from https://agupubs.onlinelibrary.wiley.com/doi/10.1029/2025JG009061 by Readcube (Labtiva Inc.), Wiley Online Library on [19/11/2026]. See the Terms and Conditions (https://onlinelibrary.wiley.com/terms-and-conditions) on Wiley Online Library for rules of use; OA articles are governed by the applicable Creative Commons License

The differences in light and nutrient availability can also influence primary production in the studied streams (Pilla & Griffiths, 2024). Previous studies have shown DOM-bound nutrients to enhance primary productivity when light availability is high, while in freshwaters with higher DOC concentrations, light availability becomes a limiting factor and results in a decrease in primary production rates, regardless of high nutrient levels (Olson et al., 2020). This pattern agrees with the higher concentrations and chromophoricity of DOC (i.e., CDOM) in the BW stream, together with the more enriched signature of δ^{13}C-CO_2.

Surprisingly, our results showed increases in the CH_4 fluxes of the CW stream during late summer and fall, being similar or even higher than in the BW stream. Previous studies have identified strong links between CH_4 production and decomposition of in situ submerged aquatic vegetation (i.e., macrophytes; Cronin et al., 2006; Marinho et al., 2015). Therefore, the seasonal increases in the CH_4 fluxes of the CW stream could be caused by the increased occurrence and decay of submerged macrophytes during baseflow conditions creating higher supply of biolabile organic carbon (OC) for anoxic sediment respiration and methanogenesis (Bastviken et al., 2023; Grasset et al., 2018; West et al., 2015; Wik et al., 2018). This possibility is also supported by an earlier study in the CW stream showing an increased abundance of benthic macrophytes coinciding with biolabile aliphatic-rich DOM signatures during baseflow (Saarela et al., 2024).

Concerning the role of microbes in the CH_4 dynamics of the studied streams, the positive correlations for CH_4 flux with methanogens (richness and diversity of *mcrA* gene) in the submerged aquatic plants further indicate benthic vegetation to be a significant contributor to autochthonous C accumulation and methanogenesis in both streams (Table S13 in Supporting Information S1). Together with *mcrA* gene diversity, *mmoX* gene richness of the aquatic plants increased with increasing CH_4 fluxes. These variables were included in model 10, suggesting that they are the most informative molecular descriptors of the CH_4 fluxes (Table 2). Resource control of functional diversity is a fundamental topic in ecology (Worm et al., 2002), and in the studied streams the positive correlations (i.e., *mcrA* diversity vs. CO_2 flux, and *mmoX* diversity vs. CH_4 flux; Table S13 in Supporting Information S1) point that these communities are still on the 'left-hand' side of the classic resource-diversity curves. Furthermore, *pmoA* and *mmoX* gene copies were also positively correlated to the CH_4 fluxes (Tables S12 and S13 in Supporting Information S1), suggesting methanotrophs grow when more CH_4 is available (Arnold et al., 2023). This implies that methanotrophs can adapt to rising CH_4 availability (Duc et al., 2010), potentially counteracting larger increases in the stream CH_4 emissions. Overall, our data suggests more genetic potential for methanotrophy than for methanogenesis in all the studied habitats, that is, submerged aquatic plants, surface sediments, and water particles. This may be because CH_4 is mainly produced in deeper sediment layers than the ones we sampled (Nagler et al., 2021) or CH_4 is coming with groundwater. Also, our data show that submerged plants and surficial sediments host more CH_4-related microbes per gram than water. This result was expected as sediments host more diverse communities than water (Gou et al., 2023). Furthermore, a low abundance of CH_4-related microbes in water is probably because these streams are not stagnant and do not have lakes upstream. Submerged aquatic plants is an overlooked habitat that seems to provide an important habitat for methanotrophs, particularly in the CW stream with higher *pmoA* amounts (gene copies per gram of plant) and higher coverage of plants (observed by ocular perception) but lower amounts of water (i.e., discharge) respect to the BW stream (supporting our hypothesis 4). However, further studies quantifying the biomass of macrophytes in lotic ecosystems are needed (Alahuhta et al., 2021) to better estimate the importance of this habitat to host methanotrophs compared with water or surface sediments. The role of aquatic plants in CH_4 cycling is better established in coastal and lentic ecosystems, where they provide suitable habitats for methanotrophs (Sorrell et al., 2002; Yoshida et al., 2014) and methanogens, the latter being restricted to more anoxic zones, such as the rhizosphere (Conrad, 2004). Submerged plants can also enhance methanotroph abundance in adjacent sediments (Zhu et al., 2023) and influence CH_4 concentrations in the water column (Theus & Holgerson, 2025). However, their role in oxic methane production remains unclear (Hilt et al., 2022).

Regarding the communities of CH_4-related microbes per se, *pmoA* and *mcrA* communities differ by habitat and time while *mmoX* community differ by stream (Figure 4). The latter supposes a difference not only in taxonomy but also in function as the genera dominating in the CW stream (Bradyrhizobium, *Paracoccus*, *Methylocella,* and *Methylibium*) harbor a propane monooxygenase (MO), that is, a close-related enzyme to the soluble CH_4 MO but without the capacity to oxidize CH_4 (Osborne & Haritos, 2019) while the genera dominating the BW stream (*Methylovulum* and *Methylomonas*) harbor soluble CH_4 MO. The more abundant CH_4-related genus, that is, the *pmoA*-harboring *Methyloglobulus* and *Methylobacter*, the above-mentioned *mmoX* genus, and the *mcrA Methanobacterium* and *Methanosaeta*, are also abundant in other river sediments, while *Methylocystis* is abundant in

other rivers but it is not in our studied streams (Burrows et al., 2021; Mo et al., 2025; Nagler et al., 2021; Oshkin et al., 2014; Sherry et al., 2016; Xing et al., 2023). Further studies quantifying CH_4 production and consumption rates and not only fluxes, and identifying active microbes, are needed to define better the role of CH_4-related microbes present within streams.

4.3. Seasonal and Hydrological Patterns Associated With C Gas Emissions

The results showed a significant seasonal variation in the fluxes of CH_4 from the BW and CW stream. The highest CH_4 fluxes from the BW stream were detected during or right after the spring freshet (May–June), whereas in the CW stream, the CH_4 fluxes peaked during late summer (July-August). The highest abundances of CH_4-related microbes for *pmoA*, *mmoX,* and *mcrA* genes were also recorded during May–June, particularly in samples from the BW stream.

We found that the seasonal differences in stream CH_4 fluxes were mainly driven by precipitation and DOC flux (dependent on DOC concentration and discharge). In streams with hydrologically connected riparian soils, strong positive correlations between CH_4 emissions and precipitation have been reported (Leng et al., 2021; Piatka et al., 2024). At rising water levels associated with spring freshet and precipitation events, high concentrations of dissolved CH_4, other C compounds and microbes can be flushed from soils and peatlands into headwater streams (Piatka et al., 2024; Ruiz-Gonzalez et al., 2015). In the BW stream, the maximum fluxes of CH_4 and DOC occurred during the spring freshet, suggesting the flux of CH_4 to be controlled by water discharge and the DOC load from the peatland dominated catchment. Compared with the CW stream, the BW stream was associated with higher and more variable discharge, which largely explains seasonal patterns of the CH_4 fluxes (Leng et al., 2021). Furthermore, CH_4 emitted from the BW stream during spring was generally more enriched in ^{13}C than CH_4 emitted later in the summer. This pattern is similar to previous studies measuring stable isotopic signatures of CH_4 in northern peatlands of Finnish Lapland (Fisher et al., 2017; Sriskantharajah et al., 2012), which further highlights that surrounding peatlands have a dominant role in defining the seasonality of stream CH_4 fluxes.

In the CW stream characterized by lower discharge and more stable baseflow compared with the BW stream, the maximum stream CH_4 fluxes detected during July and August could be attributed to the high rain events during late summer. This is also evidenced by a strong positive relationship between CH_4 flux and precipitation. Previous studies show that the seasonal maximum in C gas fluxes can occur within 3 weeks after heavy rain events in the summer (Ojala et al., 2011). On the other hand, groundwater can be an important source of CH_4 to Arctic freshwaters, and recent studies have found higher CH_4 fluxes and more depleted isotopic signatures of $\delta^{13}C$-CH_4 in groundwater compared with surface water (Dabrowski et al., 2020). Therefore, the increased CH_4 fluxes from the CW stream during late summer, together with the depleted $\delta^{13}C$-CH_4 signature, might also be linked to CH_4 inputs from groundwater.

In addition to seasonal variation, we found evidence of inter-annual variability in the CH_4 fluxes from the CW stream, where the CH_4 fluxes were significantly higher in 2022 compared with 2023. The warmer and rainier year 2022 displayed higher daily discharge in the CW stream during the sampling occasions from June to August compared with the year 2023. These findings are consistent with earlier studies in boreal lakes showing increases in C gas concentrations and fluxes as a consequence of high precipitation (Lopéz Bellido et al., 2013; Ojala et al., 2011).

The seasonal variability in the CO_2 fluxes showed a similar pattern in both the BW and CW stream, with the elevated CO_2 fluxes detected during the spring freshet. The strong positive relationships for the CO_2 flux with discharge and precipitation indicate that the seasonality in the CO_2 fluxes was strongly driven by hydrological variability. While some northern streams exhibit decreased stream CO_2 fluxes during the spring freshet, possibly due to dilution effect by the increased water inputs from snow melt and rain events (Dinsmore et al., 2011; Dyson et al., 2011; Miettinen et al., 2020), our results in contrast suggest that the spring flood flushes terrestrial C to the streams via surface flow, leading to enhanced CO_2 release to the atmosphere. The positive relationship between the fluxes of CO_2 and DOC further supports this conclusion, implying that increased export of DOC enabled efficient OC mineralization to CO_2 in the streams during spring. This agrees with seasonal patterns observed earlier, for example, in Siberian Arctic rivers (Krickov et al., 2023), and suggests that the spring freshet is not only a major period of DOC export but also a dominant component of the annual CO_2 evasion to the atmosphere.

21698961, 2026, 1, Downloaded from https://agupubs.onlinelibrary.wiley.com/doi/10.1029/2025JG009061 by Readcube (Labtiva Inc.), Wiley Online Library on [19/11/2026]. See the Terms and Conditions (https://onlinelibrary.wiley.com/terms-and-conditions) on Wiley Online Library for rules of use; OA articles are governed by the applicable Creative Commons License

21698961, 2026, 1, Downloaded from https://agupubs.onlinelibrary.wiley.com/doi/10.1029/2025JG009061 by Readcube (Labtiva Inc.), Wiley Online Library on [19/11/2026]. See the Terms and Conditions (https://onlinelibrary.wiley.com/terms-and-conditions) on Wiley Online Library for rules of use; OA articles are governed by the applicable Creative Commons License

Surprisingly, after a decline in the CO_2 fluxes from spring to summer, there was an increase in the CO_2 fluxes of the two streams during October in both sampling years. In October 2022, chloride (Cl^-) concentrations clearly increased in both streams. Since groundwater typically has higher Cl^- concentrations compared to surface water due to Cl^- accumulating from mineral dissolution, these increases could imply CO_2 inputs from groundwater into the streams under base flow conditions (Dawson et al., 2001). Furthermore, while we did not find a similar increase in Cl^- concentrations during October 2023, water discharge increased in both streams during October 2023 prior to sampling. Therefore, it is likely that the elevated stream CO_2 fluxes during late autumn were linked to shifts in flow path behavior.

Seasonal variation in C gas fluxes was evident in this study. The results indicate that the monthly variation in the CH_4 and CO_2 fluxes was clearly attributed to changes in water discharge, precipitation, and DOC export, supporting our third hypothesis. While the CH_4 and CO_2 fluxes were strongly determined by catchment hydrology and DOC dynamics during spring, groundwater inputs could have an important influence on stream C gas fluxes during low flow conditions (hypothesis 2). While we did not find evidence of inter-annual variation in C gas fluxes from the BW stream, the CW stream displayed significantly higher CH_4 fluxes in 2022 compared with 2023. Our results suggest that shifting precipitation patterns and subsequent flooding might notably alter the seasonal and inter-annual CH_4 release from small streams draining upland forest catchments. While northern peatland catchments and their CH_4 cycling are known to be highly vulnerable to hydrologic and climatic changes (Hugelius et al., 2020; Kokkonen et al., 2019), this study also provides important insights into the seasonal CH_4 dynamics of subarctic streams in upland forest ecosystems.

5. Conclusions

This study identifies catchment characteristics and seasonal patterns associated with CH_4 and CO_2 emissions from subarctic streams by conducting 2-year flux measurements and stable isotopic analyses of CH_4 and CO_2 in two contrasting catchments. The results demonstrate significantly higher C gas fluxes from the BW stream surrounded by peatlands. The CH_4 and CO_2 fluxes were positively related to terrestrial DOC export, highlighting that land cover has a major role in regulating the stream C gas fluxes. The results also show that submerged aquatic vegetation may significantly contribute to the CH_4 cycling of subarctic streams by providing a suitable habitat for methanotrophic microbes. Methanotrophs, particularly *pmoA*-harboring microbes, were more abundant than methanogens in all studied habitats. Overall, the abundance of CH_4-related microbes peaked with the maximum CH_4 fluxes, and their communities were similar in both streams. The seasonal variability in the CH_4 and CO_2 fluxes was strongly linked to changes in water discharge, precipitation, and DOC export. Simultaneously with elevated DOC load from the catchment, the stream CO_2 fluxes clearly peaked during the spring flood. This suggests that the spring freshet is not only a dominant period of DOC export but also has a major role in the annual CO_2 release from subarctic streams to the atmosphere. The CH_4 dynamics exhibited contrasting seasonal patterns between the two streams. In the BW stream, the maximum CH_4 fluxes also occurred during the spring freshet, indicating that the CH_4 fluxes were influenced by surface flow paths and DOC load from peatlands. In contrast, in the CW stream, the peak CH_4 fluxes observed in late summer could be linked to rainfall events, shifting hydrological pathways during baseflow, and to microbial decomposition of decaying aquatic plants. The interannual differences in the CH_4 fluxes from the CW stream might indicate that rain events and subsequent flooding can notably alter CH_4 release from streams to the atmosphere. This elucidates that freshwaters draining upland forest catchments might be highly sensitive to hydrological changes in a changing climate.

Conflict of Interest

The authors declare no conflicts of interest relevant to this study.

Data Availability Statement

The data used in this study are available at Zenodo via https://doi.org/10.5281/zenodo.15309570 with the license CC BY 4.0 (Saarela et al., 2025). Similarly, the sequences are available in the NCBI Sequence Read Archive (PRJNA1261814). Meteorological data used in this study are available at SmartSMEAR via https://smear.avaa.csc.fi/download (stations SMEAR I Värriö forest and SMEAR I Nuorttiaapa wetland) with the license CC BY 4.0.

Acknowledgments
This research was funded by Finnish Cultural Foundation (TS), the Academy of Finland projects CASCAS (no 14565), RIVERVOC (no 355847), and SERVICO2 (no 367821), and The ACCC Flagship funded by the Academy of Finland (no 337550, 357905, 359343). The work of MEM was supported by the Academy of Finland projects Thaw-N (no 349503) and PANDA (317054). The work of HMPS was supported by the Academy of Finland project NitroBiome (no 342362). We thank Anne Kuningas, Niko Kinnunen, Jessenia Polack, Mathilde Rebiffé, and Huizhong Zhang-Turpeinen for help in field work and laboratory analyses; and Benoit Demars for macrophyte identification. Open access publishing facilitated by Ita-Suomen yliopisto, as part of the Wiley - FinELib agreement.

References

Ågren, G. I., Bosatta, E., & Balesdent, J. (1996). Isotope discrimination during decomposition of organic matter: A theoretical analysis. *Soil Science Society of America Journal*, *60*(4), 1121–1126. https://doi.org/10.2136/sssaj1996.03615995006000040023x

Alahuhta, J., Lindholm, M., Baastrup-Spohr, L., García-Girón, J., Toivanen, M., Heino, J., & Murphy, K. (2021). Macroecology of macrophytes in the freshwater realm: Patterns, mechanisms and implications. *Aquatic Botany*, *168*, 103325. https://doi.org/10.1016/j.aquabot.2020.103325

Arnold, W., Taylor, M., Bradford, M., Raymond, P., & Peccia, J. (2023). Microbial activity contributes to spatial heterogeneity of wetland methane fluxes. *Microbiology Spectrum*, *11*(5), e02714-23. https://doi.org/10.1128/spectrum.02714-23

Asmala, E., Carstensen, J., & Räike, A. (2019). Multiple anthropogenic drivers behind upward trends in organic carbon concentrations in boreal Rivers. *Environmental Research Letters*, *14*(12), 124018. https://doi.org/10.1088/1748-9326/ab4fa9

Barker, J. F., & Fritz, P. (1981). Carbon isotope fractionation during microbial methane oxidation. *Nature*, *293*(5830), 289–291. https://doi.org/10.1038/293289a0

Bastviken, D., Santoro, A. L., Marotta, H., Pinho, L. Q., Calheiros, D. F., Crill, P., & Enrich-Prast, A. (2010). Methane emissions from pantanal, South America, during the low water season: Toward more comprehensive sampling. *Environmental Science & Technology*, *44*(14), 5450–5455. https://doi.org/10.1021/es1005048

Bastviken, D., Treat, C. C., Pangala, S. R., Gauci, V., Enrich-Prast, A., Karlson, M., et al. (2023). The importance of plants for methane emission at the ecosystem scale. *Aquatic Botany*, *184*, 103596. https://doi.org/10.1016/j.aquabot.2022.103596

Bayer, T. K., Gustafsson, E., Brakebusch, M., & Beer, C. (2019). Future carbon emission from boreal and permafrost Lakes are sensitive to catchment organic carbon loads. *Journal of Geophysical Research: Biogeosciences*, *124*(7), 1827–1848. https://doi.org/10.1029/2018JG004978

Berberich, M. E., Beaulieu, J. J., Hamilton, T. L., Waldo, S., & Buffam, I. (2020). Spatial variability of sediment methane production and methanogen communities within a eutrophic reservoir: Importance of organic matter source and quantity. *Limnology & Oceanography*, *65*(6), 1336–1358. https://doi.org/10.1002/lno.11392

Berggren, M., & Del Giorgio, P. A. (2015). Distinct patterns of microbial metabolism associated to riverine dissolved organic carbon of different source and quality. *Journal of Geophysical Research: Biogeosciences*, *120*(6), 989–999. https://doi.org/10.1002/2015JG002963

Berggren, M., Guillemette, F., Bieroza, M., Buffam, I., Deininger, A., Hawkes, J. A., et al. (2022). Unified understanding of intrinsic and extrinsic controls of dissolved organic carbon reactivity in aquatic ecosystems. *Ecology*, *103*(9), e3763. https://doi.org/10.1002/ecy.3763

Berggren, M., Laudon, H., & Jansson, M. (2007). Landscape regulation of bacterial growth efficiency in boreal freshwaters. *Global Biogeochemical Cycles*, *21*(4), 2006GB002844. https://doi.org/10.1029/2006GB002844

Biehler, A., Buffin-Bélanger, T., Baudron, P., & Chaillou, G. (2023). Groundwater discharge contribution to dissolved inorganic carbon and riverine carbon emissions in a subarctic region. *Biogeochemistry*, *165*(2), 129–150. https://doi.org/10.1007/s10533-023-01060-9

Bradshaw, C. J. A., & Warkentin, I. G. (2015). Global estimates of boreal forest carbon stocks and flux. *Global and Planetary Change*, *128*, 24–30. https://doi.org/10.1016/j.gloplacha.2015.02.004

Burrows, R. M., van de Kamp, J., Bodrossy, L., Venarsky, M., Coates-Marnane, J., Rees, G., et al. (2021). Methanotroph community structure and processes in an inland river affected by natural gas macro-seeps. *FEMS Microbiology Ecology*, *97*(10), fiab130. https://doi.org/10.1093/femsec/fiab130

Campeau, A., Bishop, K., Nilsson, M. B., Klemedtsson, L., Laudon, H., Leith, F. I., et al. (2018). Stable carbon isotopes reveal soil-stream DIC linkages in contrasting headwater catchments. *Journal of Geophysical Research: Biogeosciences*, *123*(1), 149–167. https://doi.org/10.1002/2017JG004083

Campeau, A., Wallin, M. B., Giesler, R., Löfgren, S., Mörth, C.-M., Schiff, S., et al. (2017). Multiple sources and sinks of dissolved inorganic carbon across Swedish streams, refocusing the lens of stable C isotopes. *Scientific Reports*, *7*(1), 9158. https://doi.org/10.1038/s41598-017-09049-9

Chanton, J., Chaser, L., Glasser, P., & Siegel, D. (2005). Carbon and hydrogen isotopic effects in microbial, methane from terrestrial environments. In *Stable isotopes and biosphere atmosphere interactions* (pp. 85–105). Elsevier. https://doi.org/10.1016/B978-012088447-6/50006-4

Chanton, J. P. (2005). The effect of gas transport on the isotope signature of methane in wetlands. *Organic Geochemistry*, *36*(5), 753–768. https://doi.org/10.1016/j.orggeochem.2004.10.007

Chaudhary, P. P., Rulík, M., & Blaser, M. (2017). Is the methanogenic community reflecting the methane emissions of river sediments? Comparison of two study sites. *MicrobiologyOpen*, *6*(4), e00454. https://doi.org/10.1002/mbo3.454

Coleman, M. L., & Raiswell, R. (1981). Carbon, oxygen and sulphur isotope variations in concretions from the upper lias of N.E. England. *Geochimica et Cosmochimica Acta*, *45*(3), 329–340. https://doi.org/10.1016/0016-7037(81)90243-X

Connolly, C. T., Cardenas, M. B., Burkart, G. A., Spencer, R. G. M., & McClelland, J. W. (2020). Groundwater as a major source of dissolved organic matter to arctic coastal waters. *Nature Communications*, *11*(1), 1479. https://doi.org/10.1038/s41467-020-15250-8

Conrad, R. (2004). Methanogenic microbial communities associated with aquatic plants. In A. Varma, L. Abbott, D. Werner, & R. Hampp (Eds.), *Plant surface microbiology* (pp. 35–50). Springer.

Conrad, R. (2005). Quantification of methanogenic pathways using stable carbon isotopic signatures: A review and a proposal. *Organic Geochemistry*, *36*(5), 739–752. https://doi.org/10.1016/j.orggeochem.2004.09.006

Cory, R. M., Crump, B. C., Dobkowski, J. A., & Kling, G. W. (2013). Surface exposure to sunlight stimulates CO_2 release from permafrost soil carbon in the arctic. *Proceedings of the National Academy of Sciences*, *110*(9), 3429–3434. https://doi.org/10.1073/pnas.1214104110

Cronin, G., Lewis, W. M., & Schiehser, M. A. (2006). Influence of freshwater macrophytes on the Littoral ecosystem structure and function of a young Colorado reservoir. *Aquatic Botany*, *85*(1), 37–43. https://doi.org/10.1016/j.aquabot.2006.01.011

Dabrowski, J. S., Charette, M. A., Mann, P. J., Ludwig, S. M., Natali, S. M., Holmes, R. M., et al. (2020). Using radon to quantify groundwater discharge and methane fluxes to a shallow, tundra Lake on the Yukon-Kuskokwim Delta, Alaska. *Biogeochemistry*, *148*(1), 69–89. https://doi.org/10.1007/s10533-020-00647-w

Dawson, J. J. C., Bakewell, C., & Billett, M. F. (2001). Is in-stream processing an important control on spatial changes in carbon fluxes in headwater catchments? *Science of The Total Environment*, *265*(1–3), 153–167. https://doi.org/10.1016/S0048-9697(00)00656-2

Dinsmore, K. J., Billett, M. F., Dyson, K. E., Harvey, F., Thomson, A. M., Piirainen, S., & Kortelainen, P. (2011). Stream water hydrochemistry as an indicator of carbon flow paths in Finnish peatland catchments during a spring snowmelt event. *Science of The Total Environment*, *409*(22), 4858–4867. https://doi.org/10.1016/j.scitotenv.2011.07.063

Dinsmore, K. J., Billett, M. F., Skiba, U. M., Rees, R. M., Drewer, J., & Helfter, C. (2010). Role of the aquatic pathway in the carbon and greenhouse gas budgets of a peatland catchment. *Global Change Biology*, *16*(10), 2750–2762. https://doi.org/10.1111/j.1365-2486.2009.02119.x

21698961, 2026, 1, Downloaded from https://agupubs.onlinelibrary.wiley.com/doi/10.1029/2025JG009061 by Readcube (Labtiva Inc.), Wiley Online Library on [19/11/2026]. See the Terms and Conditions (https://onlinelibrary.wiley.com/terms-and-conditions) on Wiley Online Library for rules of use; OA articles are governed by the applicable Creative Commons License

Dorrepaal, E., Toet, S., Van Logtestijn, R. S. P., Swart, E., Van De Weg, M. J., Callaghan, T. V., & Aerts, R. (2009). Carbon respiration from subsurface peat accelerated by climate warming in the subarctic. *Nature*, *460*(7255), 616–619. https://doi.org/10.1038/nature08216

Drake, T. W., Raymond, P. A., & Spencer, R. G. M. (2018). Terrestrial carbon inputs to inland waters: A current synthesis of estimates and uncertainty. *Limnology and Oceanography Letters*, *3*(3), 132–142. https://doi.org/10.1002/lol2.10055

Duc, N. T., Crill, P., & Bastviken, D. (2010). Implications of temperature and sediment characteristics on methane formation and oxidation in lake sediments. *Biogeochemistry*, *100*(1–3), 185–196. https://doi.org/10.1007/s10533-010-9415-8

Dumont, M. G., & Murrell, J. C. (2005). Community-Level analysis: Key genes of aerobic methane oxidation. In *Methods in Enzymology* (Vol. 397, pp. 413–427). Elsevier. https://doi.org/10.1016/S0076-6879(05)97025-0

Duvert, C., Butman, D. E., Marx, A., Ribolzi, O., & Hutley, L. B. (2018). CO_2 evasion along streams driven by groundwater inputs and geomorphic controls. *Nature Geoscience*, *11*(11), 813–818. https://doi.org/10.1038/s41561-018-0245-y

Dyson, K. E., Billett, M. F., Dinsmore, K. J., Harvey, F., Thomson, A. M., Piirainen, S., & Kortelainen, P. (2011). Release of aquatic carbon from two peatland catchments in E. Finland during the spring snowmelt period. *Biogeochemistry*, *103*(1–3), 125–142. https://doi.org/10.1007/s10533-010-9452-3

Eddy, S. R. (2022). *HMMER: Biosequence analysis using profile hidden Markov models*. Howard Hughes Medical Institute. Retrieved from http://hmmer.org

Erkkilä, K.-M., Ojala, A., Bastviken, D., Biermann, T., Heiskanen, J. J., Lindroth, A., et al. (2018). Methane and carbon dioxide fluxes over a Lake: Comparison between eddy covariance, floating chambers and boundary layer method. *Biogeosciences*, *15*(2), 429–445. https://doi.org/10.5194/bg-15-429-2018

Fellman, J. B., D'Amore, D. V., Hood, E., & Boone, R. D. (2008). Fluorescence characteristics and biodegradability of dissolved organic matter in forest and wetland soils from coastal temperate watersheds in southeast Alaska. *Biogeochemistry*, *88*(2), 169–184. https://doi.org/10.1007/s10533-008-9203-x

Finlay, J., Neff, J., Zimov, S., Davydova, A., & Davydov, S. (2006). Snowmelt dominance of dissolved organic carbon in high-latitude watersheds: Implications for characterization and flux of river DOC. *Geophysical Research Letters*, *33*(10), 2006GL025754. https://doi.org/10.1029/2006GL025754

Finstad, A. G., Andersen, T., Larsen, S., Tominaga, K., Blumentrath, S., De Wit, H. A., et al. (2016). From greening to browning: Catchment vegetation development and reduced S-deposition promote organic carbon load on decadal time scales in Nordic Lakes. *Scientific Reports*, *6*(1), 31944. https://doi.org/10.1038/srep31944

Fisher, R. E., France, J. L., Lowry, D., Lanoisellé, M., Brownlow, R., Pyle, J. A., et al. (2017). Measurement of the ^{13}C isotopic signature of methane emissions from northern European wetlands. *Global Biogeochemical Cycles*, *31*(3), 605–623. https://doi.org/10.1002/2016GB005504

Fouché, J., Lafrenière, M. J., Rutherford, K., & Lamoureux, S. (2017). Seasonal hydrology and permafrost disturbance impacts on dissolved organic matter composition in high arctic headwater catchments. *Arctic Science*, *3*(2), 378–405. https://doi.org/10.1139/as-2016-0031

Friedrich, M. W. (2005). Methyl-coenzyme M reductase genes: Unique functional markers for methanogenic and anaerobic methane-oxidizing archaea. In *Methods in Enzymology* (Vol. 397, pp. 428–442). Elsevier. https://doi.org/10.1016/S0076-6879(05)97026-2

Gålfalk, M., Bastviken, D., Fredriksson, S., & Arneborg, L. (2013). Determination of the piston velocity for water-air interfaces using flux chambers, acoustic Doppler velocimetry, and IR imaging of the water surface. *Journal of Geophysical Research: Biogeosciences*, *118*(2), 770–782. https://doi.org/10.1002/jgrg.20064

Ge, M., Korrensalo, A., Putkinen, A., Laiho, R., Kohl, L., Pihlatie, M., et al. (2025). CH_4 transport in wetland plants under controlled environmental conditions–Separating the impacts of phenology from environmental variables. *Plant and Soil*, *507*(1–2), 671–691. https://doi.org/10.1007/s11104-024-06756-x

Gómez-Gener, L., Rocher-Ros, G., Battin, T., Cohen, M. J., Dalmagro, H. J., Dinsmore, K. J., et al. (2021). Global carbon dioxide efflux from Rivers enhanced by high nocturnal emissions. *Nature Geoscience*, *14*(5), 289–294. https://doi.org/10.1038/s41561-021-00722-3

Gou, Y., Qin, Y., Ouyang, C., Zheng, W., & Jiang, C. (2023). Research on aerobic oxidation of methane bacteria and its influencing factors in Chongqing central city section of the Yangtze river, China. *Environmental Geochemistry and Health*, *45*(8), 6435–6453. https://doi.org/10.1007/s10653-023-01631-7

Graham, E. B., Knelman, J. E., Schindlbacher, A., Siciliano, S., Breulmann, M., Yannarell, A., et al. (2016). Microbes as engines of ecosystem function: When does community structure enhance predictions of ecosystem processes? *Frontiers in Microbiology*, *7*, 214. https://doi.org/10.3389/fmicb.2016.00214

Grasset, C., Mendonça, R., Villamor Saucedo, G., Bastviken, D., Roland, F., & Sobek, S. (2018). Large but variable methane production in anoxic freshwater sediment upon addition of allochthonous and autochthonous organic matter. *Limnology & Oceanography*, *63*(4), 1488–1501. https://doi.org/10.1002/lno.10786

Guillemette, F., McCallister, S. L., & Del Giorgio, P. A. (2013). Differentiating the degradation dynamics of algal and terrestrial carbon within complex natural dissolved organic carbon in temperate Lakes. *Journal of Geophysical Research: Biogeosciences*, *118*(3), 963–973. https://doi.org/10.1002/jgrg.20077

Guo, L., Ping, C., & Macdonald, R. W. (2007). Mobilization pathways of organic carbon from permafrost to arctic Rivers in a changing climate. *Geophysical Research Letters*, *34*(13), 2007GL030689. https://doi.org/10.1029/2007GL030689

Hilt, S., Grossart, H., McGinnis, D. F., & Keppler, F. (2022). Potential role of submerged macrophytes for oxic methane production in aquatic ecosystems. *Limnology & Oceanography*, *67*(S2), S76–S88. https://doi.org/10.1002/lno.12095

Hu, C., Muller-Karger, F. E., & Zepp, R. G. (2002). Absorbance, absorption coefficient, and apparent quantum yield: A comment on common ambiguity in the use of these optical concepts. *Limnology & Oceanography*, *47*(4), 1261–1267. https://doi.org/10.4319/lo.2002.47.4.1261

Hugelius, G., Loisel, J., Chadburn, S., Jackson, R. B., Jones, M., MacDonald, G., et al. (2020). Large stocks of peatland carbon and nitrogen are vulnerable to permafrost thaw. *Proceedings of the National Academy of Sciences*, *117*(34), 20438–20446. https://doi.org/10.1073/pnas.1916387117

Huotari, J., Nykänen, H., Forsius, M., & Arvola, L. (2013). Effect of catchment characteristics on aquatic carbon export from a boreal catchment and its importance in regional carbon cycling. *Global Change Biology*, *19*(12), 3607–3620. https://doi.org/10.1111/gcb.12333

Jentzsch, K., Männistö, E., Marushchak, M. E., Korrensalo, A., Van Delden, L., Tuittila, E.-S., et al. (2024). Seasonal controls on methane flux components in a boreal peatland – Combining plant removal and stable isotope analyses. *EGUsphere*, *2024*, 1–32. https://doi.org/10.5194/egusphere-2023-3098

Johnston, S. E., Carey, J. C., Kellerman, A., Podgorski, D. C., Gewirtzman, J., & Spencer, R. G. M. (2021). Controls on riverine dissolved organic matter composition across an arctic-boreal latitudinal gradient. *Journal of Geophysical Research: Biogeosciences*, *126*(9), e2020JG005988. https://doi.org/10.1029/2020JG005988

21698961, 2026, 1, Downloaded from https://agupubs.onlinelibrary.wiley.com/doi/10.1029/2025JG009061 by Readcube (Labtiva Inc.), Wiley Online Library on [19/11/2026]. See the Terms and Conditions (https://onlinelibrary.wiley.com/terms-and-conditions) on Wiley Online Library for rules of use; OA articles are governed by the applicable Creative Commons License

Juutinen, S., Väliranta, M., Kuutti, V., Laine, A. M., Virtanen, T., Seppä, H., et al. (2013). Short-term and long-term carbon dynamics in a northern peatland-stream-lake continuum: A catchment approach. *Journal of Geophysical Research: Biogeosciences*, *118*(1), 171–183. https://doi.org/10.1002/jgrg.20028

Karlsson, J., Jansson, M., & Jonsson, A. (2007). Respiration of allochthonous organic carbon in unproductive forest Lakes determined by the keeling plot method. *Limnology & Oceanography*, *52*(2), 603–608. https://doi.org/10.4319/lo.2007.52.2.0603

Katoh, K., & Standley, D. M. (2013). MAFFT multiple sequence alignment software version 7: Improvements in performance and usability. *Molecular Biology and Evolution*, *30*(4), 772–780. https://doi.org/10.1093/molbev/mst010

Kawahigashi, M., Kaiser, K., Rodionov, A., & Guggenberger, G. (2006). Sorption of dissolved organic matter by mineral soils of the Siberian forest tundra. *Global Change Biology*, *12*(10), 1868–1877. https://doi.org/10.1111/j.1365-2486.2006.01203.x

Kokkonen, N. A. K., Laine, A. M., Laine, J., Vasander, H., Kurki, K., Gong, J., & Tuittila, E. (2019). Responses of peatland vegetation to 15-year water level drawdown as mediated by fertility level. *Journal of Vegetation Science*, *30*(6), 1206–1216. https://doi.org/10.1111/jvs.12794

Kolb, S., Knief, C., Stubner, S., & Conrad, R. (2003). Quantitative detection of methanotrophs in soil by novel *pmoA* -Targeted real-time PCR assays. *Applied and Environmental Microbiology*, *69*(5), 2423–2429. https://doi.org/10.1128/AEM.69.5.2423-2429.2003

Korhonen, J., & Haavanlammi, E. (2012). *Hydrological yearbook 2006– 2010, Finnish environmental institute*. The Finnish Environment 8/2012, 2012.

Krickov, I. V., Lim, A. G., Shirokova, L. S., Korets, M. A., Karlsson, J., & Pokrovsky, O. S. (2023). Environmental controllers for carbon emission and concentration patterns in Siberian Rivers during different seasons. *Science of The Total Environment*, *859*, 160202. https://doi.org/10.1016/j.scitotenv.2022.160202

Kuivila, K. M., Murray, J. W., Devol, A. H., & Novelli, P. C. (1989). Methane production, sulfate reduction and competition for substrates in the sediments of Lake Washington. *Geochimica et Cosmochimica Acta*, *53*(2), 409–416. https://doi.org/10.1016/0016-7037(89)90392-X

Lapierre, J.-F., Guillemette, F., Berggren, M., & Del Giorgio, P. A. (2013). Increases in terrestrially derived carbon stimulate organic carbon processing and CO_2 emissions in boreal aquatic ecosystems. *Nature Communications*, *4*(1), 2972. https://doi.org/10.1038/ncomms3972

Laudon, H., Berggren, M., Ågren, A., Buffam, I., Bishop, K., Grabs, T., et al. (2011). Patterns and dynamics of dissolved organic carbon (DOC) in boreal streams: The role of processes, connectivity, and scaling. *Ecosystems*, *14*(6), 880–893. https://doi.org/10.1007/s10021-011-9452-8

Legendre, P., & Gallagher, E. D. (2001). Ecologically meaningful transformations for ordination of species data. *Oecologia*, *129*(2), 271–280. https://doi.org/10.1007/s004420100716

Leng, P., Kamjunke, N., Li, F., & Koschorreck, M. (2021). Temporal patterns of methane emissions from two streams with different riparian connectivity. *Journal of Geophysical Research: Biogeosciences*, *126*(8), e2020JG006104. https://doi.org/10.1029/2020JG006104

Letunic, I., & Bork, P. (2024). Interactive tree of life (iTOL) v6: Recent updates to the phylogenetic tree display and annotation tool. *Nucleic Acids Research*, *52*(W1), W78–W82. https://doi.org/10.1093/nar/gkae268

Levine, U. Y., Teal, T. K., Robertson, G. P., & Schmidt, T. M. (2011). Agriculture's impact on microbial diversity and associated fluxes of carbon dioxide and methane. *The ISME Journal*, *5*(10), 1683–1691. https://doi.org/10.1038/ismej.2011.40

López Bellido, J., Tulonen, T., Kankaala, P., & Ojala, A. (2013). Concentrations of CO_2 and CH_4 in water columns of two stratified boreal Lakes during a year of atypical summer precipitation. *Biogeochemistry*, *113*(1–3), 613–627. https://doi.org/10.1007/s10533-012-9792-2

Lundin, E. J., Giesler, R., Persson, A., Thompson, M. S., & Karlsson, J. (2013). Integrating carbon emissions from Lakes and streams in a subarctic catchment. *Journal of Geophysical Research: Biogeosciences*, *118*(3), 1200–1207. https://doi.org/10.1002/jgrg.20092

Lupon, A., Denfeld, B. A., Laudon, H., Leach, J., Karlsson, J., & Sponseller, R. A. (2019). Groundwater inflows control patterns and sources of greenhouse gas emissions from streams. *Limnology & Oceanography*, *64*(4), 1545–1557. https://doi.org/10.1002/lno.11134

Marinho, C. C., Palma-Silva, C., Albertoni, E. F., Giacomini, I. B., Barros, M. P. F., Furlanetto, L. M., & Esteves, F. D. A. (2015). Emergent macrophytes alter the sediment composition in a small, shallow subtropical Lake: Implications for methane emission. *American Journal of Plant Sciences*, *6*(2), 315–322. https://doi.org/10.4236/ajps.2015.62036

McClelland, J. W., Déry, S. J., Peterson, B. J., Holmes, R. M., & Wood, E. F. (2006). A pan-arctic evaluation of changes in river discharge during the latter half of the 20th century. *Geophysical Research Letters*, *33*(6), 2006GL025753. https://doi.org/10.1029/2006GL025753

McDonald, I. R., & Murrell, J. C. (1997). The particulate methane monooxygenase gene pmoA and its use as a functional gene probe for methanotrophs. *FEMS Microbiology Letters*, *156*(2), 205–210. https://doi.org/10.1111/j.1574-6968.1997.tb12728.x

McDonough, L. K., Andersen, M. S., Behnke, M. I., Rutlidge, H., Oudone, P., Meredith, K., et al. (2022). A new conceptual framework for the transformation of groundwater dissolved organic matter. *Nature Communications*, *13*(1), 2153. https://doi.org/10.1038/s41467-022-29711-9

Miettinen, H., Pumpanen, J., Rantakari, M., & Ojala, A. (2020). Carbon dynamics in a boreal land-stream-lake continuum during the spring freshet of two hydrologically contrasting years. *Biogeochemistry*, *148*(1), 91–109. https://doi.org/10.1007/s10533-020-00648-9

Mo, Y., Huang, J., Hu, M., Lu, L., & Shaaban, M. (2025). Community structure and function of aerobic methanotrophs in urban river sediments: A case study of the Jialing river. *Environmental Microbiology Reports*, *17*(4), e70167. https://doi.org/10.1111/1758-2229.70167

Monteith, D. T., Stoddard, J. L., Evans, C. D., De Wit, H. A., Forsius, M., Høgåsen, T., et al. (2007). Dissolved organic carbon trends resulting from changes in atmospheric deposition chemistry. *Nature*, *450*(7169), 537–540. https://doi.org/10.1038/nature06316

Mörth, C., Laudon, H., Mellqvist, E., Torssander, P., & Giesler, R. (2008). Sources of stream water sulfate during the spring snowmelt in boreal streams: Evidence from $\delta^{34}S$ isotope measurements. *Journal of Geophysical Research*, *113*(G1), 2007JG000457. https://doi.org/10.1029/2007JG000457

Muyzer, G., De Waal, E. C., & Uitterlinden, A. G. (1993). Profiling of complex microbial populations by denaturing gradient gel electrophoresis analysis of polymerase chain reaction-amplified genes coding for 16S rRNA. *Applied and Environmental Microbiology*, *59*(3), 695–700. https://doi.org/10.1128/aem.59.3.695-700.1993

Nagler, M., Praeg, N., Niedrist, G. H., Attermeyer, K., Catalán, N., Pilotto, F., et al. (2021). Abundance and biogeography of methanogenic and methanotrophic microorganisms across European streams. *Journal of Biogeography*, *48*(4), 947–960. https://doi.org/10.1111/jbi.14052

Natelhoffer, K. J., & Fry, B. (1988). Controls on natural Nitrogen-15 and Carbon-13 abundances in forest soil organic matter. *Soil Science Society of America Journal*, *52*(6), 1633–1640. https://doi.org/10.2136/sssaj1988.03615995005200060024x

Nguyen, L.-T., Schmidt, H. A., Von Haeseler, A., & Minh, B. Q. (2015). IQ-TREE: A fast and effective stochastic algorithm for estimating maximum-likelihood phylogenies. *Molecular Biology and Evolution*, *32*(1), 268–274. https://doi.org/10.1093/molbev/msu300

Ojala, A., Bellido, J. L., Tulonen, T., Kankaala, P., & Huotari, J. (2011). Carbon gas fluxes from a brown-water and a clear-water Lake in the boreal zone during a summer with extreme rain events. *Limnology & Oceanography*, *56*(1), 61–76. https://doi.org/10.4319/lo.2011.56.1.0061

Olefeldt, D., Roulet, N., Giesler, R., & Persson, A. (2013). Total waterborne carbon export and DOC composition from ten nested subarctic peatland catchments—Importance of peatland cover, groundwater influence, and inter-annual variability of precipitation patterns. *Hydrological Processes*, *27*(16), 2280–2294. https://doi.org/10.1002/hyp.9358

Olson, C. R., Solomon, C. T., & Jones, S. E. (2020). Shifting limitation of primary production: Experimental support for a new model in Lake ecosystems. *Ecology Letters*, *23*(12), 1800–1808. https://doi.org/10.1111/ele.13606

21698961, 2026, 1, Downloaded from https://agupubs.onlinelibrary.wiley.com/doi/10.1029/2025JG009061 by Readcube (Labtiva Inc.), Wiley Online Library on [19/11/2026]. See the Terms and Conditions (https://onlinelibrary.wiley.com/terms-and-conditions) on Wiley Online Library for rules of use; OA articles are governed by the applicable Creative Commons License

Osborne, C. D., & Haritos, V. S. (2019). Beneath the surface: Evolution of methane activity in the bacterial multicomponent monooxygenases. *Molecular Phylogenetics and Evolution*, *139*, 106527. https://doi.org/10.1016/j.ympev.2019.106527

Oshkin, I. Y., Wegner, C.-E., Lüke, C., Glagolev, M. V., Filippov, I. V., Pimenov, N. V., et al. (2014). Gammaproteobacterial methanotrophs dominate cold methane seeps in floodplains of west Siberian Rivers. *Applied and Environmental Microbiology*, *80*(19), 5944–5954. https://doi.org/10.1128/AEM.01539-14

Peterson, B. J., Holmes, R. M., McClelland, J. W., Vörösmarty, C. J., Lammers, R. B., Shiklomanov, A. I., et al. (2002). Increasing river discharge to the Arctic Ocean. *Science*, *298*(5601), 2171–2173. https://doi.org/10.1126/science.1077445

Peuravuori, J., & Pihlaja, K. (1997). Molecular size distribution and spectroscopic properties of aquatic humic substances. *Analytica Chimica Acta*, *337*(2), 133–149. https://doi.org/10.1016/S0003-2670(96)00412-6

Piatka, D. R., Nánási, R. L., Mwanake, R. M., Engelsberger, F., Willibald, G., Neidl, F., & Kiese, R. (2024). Precipitation fuels dissolved greenhouse gas (CO_2, CH_4, N_2O) dynamics in a peatland-dominated headwater stream: Results from a continuous monitoring setup. *Frontiers in Water*, *5*, 1321137. https://doi.org/10.3389/frwa.2023.1321137

Pilla, R. M., & Griffiths, N. A. (2024). Integrating reservoirs into the dissolved organic matter versus primary production paradigm: How does Chlorophyll-a change across dissolved organic carbon concentrations in reservoirs? *Ecosystems*, *27*(1), 137–150. https://doi.org/10.1007/s10021-023-00878-6

Pirinen, P., Simola, H., Aalto, J., Kaukoranta, J. P., Karlsson, P., & Ruuhela, R. (2012). *Limatological statistics of Finland 1981–2010*. In (Vol. 1). Finnish Meteorological Institute reports 2012.

Pohjonen, V., Mönkkönen, P., & Hari, P. (2008). Test of northern timber line. In H. L. K. P (Ed.), *Boreal forest and climate change* (Vol. 34, pp. 472–475). Advances in global change research.

Putkinen, A., Siljanen, H. M. P., Laihonen, A., Paasisalo, I., Porkka, K., Tiirola, M., et al. (2021). New insight to the role of microbes in the methane exchange in trees: Evidence from metagenomic sequencing. *New Phytologist*, *231*(2), 524–536. https://doi.org/10.1111/nph.17365

Rahman, M. T., Crombie, A., Chen, Y., Stralis-Pavese, N., Bodrossy, L., Meir, P., et al. (2011). Environmental distribution and abundance of the facultative methanotroph *methylocella*. *The ISME Journal*, *5*(6), 1061–1066. https://doi.org/10.1038/ismej.2010.190

Rasilo, T. (2013). *Connecting silvan and lacustrine ecosystems: Transport of carbon from forests to adjacent water bodies*. University of Helsinki.155.

Raymond, P. A., Hartmann, J., Lauerwald, R., Sobek, S., McDonald, C., Hoover, M., et al. (2013). Global carbon dioxide emissions from inland waters. *Nature*, *503*(7476), 355–359. https://doi.org/10.1038/nature12760

Reis, P. C. J., Ruiz-González, C., Crevecoeur, S., Soued, C., & Prairie, Y. T. (2020). Rapid shifts in methanotrophic bacterial communities mitigate methane emissions from a tropical hydropower reservoir and its downstream river. *Science of The Total Environment*, *748*, 141374. https://doi.org/10.1016/j.scitotenv.2020.141374

Riley, W. J., Subin, Z. M., Lawrence, D. M., Swenson, S. C., Torn, M. S., Meng, L., et al. (2011). Barriers to predicting changes in global terrestrial methane fluxes: Analyses using CLM4Me, a methane biogeochemistry model integrated in CESM. *Biogeosciences*, *8*(7), 1925–1953. https://doi.org/10.5194/bg-8-1925-2011

Roach, K. A., Winemiller, K. O., & Davis, S. E. (2014). Autochthonous production in shallow Littoral zones of five floodplain Rivers: Effects of flow, turbidity and nutrients. *Freshwater Biology*, *59*(6), 1278–1293. https://doi.org/10.1111/fwb.12347

Ruiz-González, C., Niño-García, J. P., & Del Giorgio, P. A. (2015). Terrestrial origin of bacterial communities in complex boreal freshwater networks. *Ecology Letters*, *18*(11), 1198–1206. https://doi.org/10.1111/ele.12499

Saarela, T., Palacin Lizarbe, C., Hashmi, W., Kohl, L., Marushchak, M. E., Siljanen, H., et al. (2025). Greenhouse gas flux, stable isotope, water quality and molecular data from subarctic streams, värriö, Finland (2022-2023) [Dataset]. *Zenodo*. https://doi.org/10.5281/zenodo.15309570

Saarela, T., Zhu, X., Jäntti, H., Ohashi, M., Siljanen, H., Pesonen, A., et al. (2024). The influence of dissolved organic matter composition on microbial degradation and carbon dioxide production in pristine subarctic Rivers. *Boreal Environment Research*, *29*, 131–148.

Schelker, J., Grabs, T., Bishop, K., & Laudon, H. (2013). Drivers of increased organic carbon concentrations in stream water following forest disturbance: Separating effects of changes in flow pathways and soil warming. *Journal of Geophysical Research: Biogeosciences*, *118*(4), 1814–1827. https://doi.org/10.1002/2013JG002309

Schuur, E. A. G., Vogel, J. G., Crummer, K. G., Lee, H., Sickman, J. O., & Osterkamp, T. E. (2009). The effect of permafrost thaw on old carbon release and net carbon exchange from tundra. *Nature*, *459*(7246), 556–559. https://doi.org/10.1038/nature08031

Sepulveda-Jauregui, A., Hoyos-Santillan, J., Martinez-Cruz, K., Walter Anthony, K. M., Casper, P., Belmonte-Izquierdo, Y., & Thalasso, F. (2018). Eutrophication exacerbates the impact of climate warming on Lake methane emission. *Science of The Total Environment*, *636*, 411–419. https://doi.org/10.1016/j.scitotenv.2018.04.283

Sherry, A., Osborne, K. A., Sidgwick, F. R., Gray, N. D., & Talbot, H. M. (2016). A temperate river Estuary is a sink for methanotrophs adapted to extremes of pH, temperature and salinity. *Environmental Microbiology Reports*, *8*(1), 122–131. https://doi.org/10.1111/1758-2229.12359

Shogren, A. J., Zarnetske, J. P., Abbott, B. W., Iannucci, F., & Bowden, W. B. (2020). We cannot shrug off the shoulder seasons: Addressing knowledge and data gaps in an arctic headwater. *Environmental Research Letters*, *15*(10), 104027. https://doi.org/10.1088/1748-9326/ab9d3c

Siljanen, H. M. P., Manoharan, L., Hilts, A. S., Bagnoud, A., Alves, R. J. E., Jones, C. M., et al. (2025). Targeted metagenomics using probe capture detect a larger diversity of nitrogen and methane cycling genes in complex microbial communities than traditional metagenomics. *ISME Communication*, *5*(1), ycaf183. https://doi.org/10.1093/ismeco/ycaf183

Sorrell, B. K., Downes, M. T., & Stanger, C. L. (2002). Methanotrophic bacteria and their activity on submerged aquatic macrophytes. *Aquatic Botany*, *72*(2), 107–119. https://doi.org/10.1016/S0304-3770(01)00215-7

Sriskantharajah, S., Fisher, R. E., Lowry, D., Aalto, T., Hatakka, J., Aurela, M., et al. (2012). Stable carbon isotope signatures of methane from a Finnish subarctic wetland. *Tellus B: Chemical and Physical Meteorology*, *64*(1), 18818. https://doi.org/10.3402/tellusb.v64i0.18818

Stamatakis, A. (2014). RAxML version 8: A tool for phylogenetic analysis and post-analysis of large phylogenies. *Bioinformatics*, *30*(9), 1312–1313. https://doi.org/10.1093/bioinformatics/btu033

Striegl, R. G., Dornblaser, M. M., McDonald, C. P., Rover, J. A., & Stets, E. G. (2012). Carbon dioxide and methane emissions from the yukon river system. *Global Biogeochemical Cycles*, *26*(4), 2012GB004306. https://doi.org/10.1029/2012GB004306

Susiluoto, S., Rasilo, T., Pumpanen, J., & Berninger, F. (2008). Effects of grazing on the vegetation structure and carbon dioxide exchange of a fennoscandian fell ecosystem. *Arctic Antarctic and Alpine Research*, *40*(2), 422–431. https://doi.org/10.1657/1523-0430(07-035)[SUSILUOTO]2.0.CO;2

Theus, M. E., & Holgerson, M. A. (2025). Freshwater plant communities influence water column greenhouse gases. *Aquatic Botany*, *201*, 103927. https://doi.org/10.1016/j.aquabot.2025.103927

Waldron, S., Hall, A. J., & Fallick, A. E. (1999). Enigmatic stable isotope dynamics of deep peat methane. *Global Biogeochemical Cycles*, *13*(1), 93–100. https://doi.org/10.1029/1998GB900002

21698961, 2026, 1, Downloaded from https://agupubs.onlinelibrary.wiley.com/doi/10.1029/2025JG009061 by Readcube (Labtiva Inc.), Wiley Online Library on [19/11/2026]. See the Terms and Conditions (https://onlinelibrary.wiley.com/terms-and-conditions) on Wiley Online Library for rules of use; OA articles are governed by the applicable Creative Commons License

Wallin, M. B., Grabs, T., Buffam, I., Laudon, H., Ågren, A., Öquist, M. G., & Bishop, K. (2013). Evasion of CO_2 from streams – The dominant component of the carbon export through the aquatic conduit in a boreal landscape. *Global Change Biology*, *19*(3), 785–797. https://doi.org/10.1111/gcb.12083

Walvoord, M. A., & Striegl, R. G. (2007). Increased groundwater to stream discharge from permafrost thawing in the yukon river basin: Potential impacts on lateral export of carbon and nitrogen. *Geophysical Research Letters*, *34*(12), 2007GL030216. https://doi.org/10.1029/2007GL030216

Weishaar, J. L., Aiken, G. R., Bergamaschi, B. A., Fram, M. S., Fujii, R., & Mopper, K. (2003). Evaluation of specific ultraviolet absorbance as an indicator of the chemical composition and reactivity of dissolved organic carbon. *Environmental Science & Technology*, *37*(20), 4702–4708. https://doi.org/10.1021/es030360x

West, W. E., McCarthy, S. M., & Jones, S. E. (2015). Phytoplankton lipid content influences freshwater Lake methanogenesis. *Freshwater Biology*, *60*(11), 2261–2269. https://doi.org/10.1111/fwb.12652

Whiticar, M. J. (1999). Carbon and hydrogen isotope systematics of bacterial formation and oxidation of methane. *Chemical Geology*, *161*(1–3), 291–314. https://doi.org/10.1016/S0009-2541(99)00092-3

Whiticar, M. J., Faber, E., & Schoell, M. (1986). Biogenic methane formation in marine and freshwater environments: CO2 reduction vs. acetate fermentation—Isotope evidence. *Geochimica et Cosmochimica Acta*, *50*(5), 693–709. https://doi.org/10.1016/0016-7037(86)90346-7

Wickland, K. P., Waldrop, M. P., Aiken, G. R., Koch, J. C., Jorgenson, M. T., & Striegl, R. G. (2018). Dissolved organic carbon and nitrogen release from boreal Holocene permafrost and seasonally frozen soils of Alaska. *Environmental Research Letters*, *13*(6), 065011. https://doi.org/10.1088/1748-9326/aac4ad

Wik, M., Johnson, J. E., Crill, P. M., DeStasio, J. P., Erickson, L., Halloran, M. J., et al. (2018). Sediment characteristics and methane ebullition in three subarctic Lakes. *Journal of Geophysical Research: Biogeosciences*, *123*(8), 2399–2411. https://doi.org/10.1029/2017JG004298

Winfrey, M. R., & Zeikus, J. G. (1977). Effect of sulfate on carbon and electron flow during microbial methanogenesis in freshwater sediments. *Applied and Environmental Microbiology*, *33*(2), 275–281. https://doi.org/10.1128/aem.33.2.275-281.1977

Worm, B., Lotze, H. K., Hillebrand, H., & Sommer, U. (2002). Consumer versus resource control of species diversity and ecosystem functioning. *Nature*, *417*(6891), 848–851. https://doi.org/10.1038/nature00830

Xing, C.-Y., Li, H., Li, Q., Lu, L.-H., & Li, Z. (2023). Shifts in composition and function of bacterial communities reveal the effect of small barriers on nitrous oxide and methane accumulation in fragmented Rivers. *Frontiers in Microbiology*, *14*, 1110025. https://doi.org/10.3389/fmicb.2023.1110025

Yakir, D., & Sternberg, L. D. S. L. (2000). The use of stable isotopes to study ecosystem gas exchange. *Oecologia*, *123*(3), 297–311. https://doi.org/10.1007/s004420051016

Yoshida, N., Iguchi, H., Yurimoto, H., Murakami, A., & Sakai, Y. (2014). Aquatic plant surface as a niche for methanotrophs. *Frontiers in Microbiology*, *5*, 30. https://doi.org/10.3389/fmicb.2014.00030

Zhu, J., Li, Y., Huang, M., Xu, D., Zhang, Y., Zhou, Q., et al. (2023). Restoration effects of submerged macrophytes on methane production and oxidation potential of Lake sediments. *Science of The Total Environment*, *866*, 161218. https://doi.org/10.1016/j.scitotenv.2022.161218

21698961, 2026, 1, Downloaded from https://agupubs.onlinelibrary.wiley.com/doi/10.1029/2025JG009061 by Readcube (Labtiva Inc.), Wiley Online Library on [19/11/2026]. See the Terms and Conditions (https://onlinelibrary.wiley.com/terms-and-conditions) on Wiley Online Library for rules of use; OA articles are governed by the applicable Creative Commons License